

Review

Selected Worldwide Cases of Land Subsidence Due to Groundwater Withdrawal

Ploutarchos Tzampoglou ^{1,*} , Ioanna Ilia ^{2,*} , Konstantinos Karalis ³ , Paraskevas Tsangaratos ² , Xia Zhao ⁴  and Wei Chen ⁴

¹ Department of Civil & Environmental Engineering, University of Cyprus, 1678 Nicosia, Cyprus

² Laboratory of Engineering Geology and Hydrogeology, Department of Geological Sciences, School of Mining and Metallurgical Engineering, National Technical University of Athens, Zographou Campus, 157 73 Athens, Greece

³ Institute of Geological Sciences, University of Bern, 3012 Bern, Switzerland

⁴ College of Geology and Environment, Xi'an University of Science and Technology, Xi'an 710054, China

* Correspondence: tzampoglou.ploutarchos@ucy.ac.cy (P.T.); gilia@metal.ntua.gr (I.I.)

Abstract: The present review paper focuses on selected cases around the world of land subsidence phenomena caused by the overexploitation of aquifers. Land subsidence is closely related to human activity. In particular, the development of technology has led to an exponential increase in industrial and agricultural production, as well as extensive urbanization, mainly in large cities. The action of those parameters, along with the effects of climate change, has led to further increases in water demands, which have mainly been served by overexploitation of the aquifers. Overexploitation, in conjunction with broader geo-tectonic conditions, can trigger severe land subsidence phenomena, resulting in significant damage affecting the physical and man-made environment. The scope of the present study is to provide a critical review of the existing literature on land subsidence due to aquifer overexploitation and highlight the main causal factors driving this process. The methods developed in the past and their outcomes hold significant importance in sustainable development strategic planning.

Keywords: land subsidence; aquifer overexploitation; disaster response; natural hazard; literature review



Citation: Tzampoglou, P.; Ilia, I.; Karalis, K.; Tsangaratos, P.; Zhao, X.; Chen, W. Selected Worldwide Cases of Land Subsidence Due to Groundwater Withdrawal. *Water* **2023**, *15*, 1094. <https://doi.org/10.3390/w15061094>

Academic Editors: Achim A. Beylich and Adriana Bruggeman

Received: 2 February 2023

Revised: 27 February 2023

Accepted: 7 March 2023

Published: 13 March 2023



Copyright: © 2023 by the authors. Licensee MDPI, Basel, Switzerland. This article is an open access article distributed under the terms and conditions of the Creative Commons Attribution (CC BY) license (<https://creativecommons.org/licenses/by/4.0/>).

1. Introduction

Land subsidence is defined as an endogenous phenomenon caused by differential vertical displacements of the Earth's surface due to either natural or anthropogenic factors [1–4]. This process is mainly affected by the hydrological, geological, and tectonic conditions of the wider area, as well as by the geotechnical characteristics of subsurface formations. Subsidence can be triggered by the consolidation of formations by overexploitation of aquifers [5–7] or natural gas and oil [8], sinkhole collapse [9–11], oxidation of organic soils [12] or the collapse of underground mining cavities [13–16].

The mechanism behind land subsidence phenomena caused by overexploitation of aquifers is based on the principle of effective stress, which states that when a saturated soil is subjected to total stress σ , this stress can be expressed by the following equation [17]:

$$\sigma = \sigma' + u$$

where u is the pressure acting on the water and the granular structure, and σ' is the effective stress supported by the granular structure only.

A decrease in the pore water pressure and an increase in the normal effective stress are aftereffects of the incidence of excessive groundwater withdrawal from aquifer systems. The evolution of this process results in the compaction of the hydrostratigraphic units, which eventually leads to land subsidence [18,19].

During the 20th century, subsidence was observed in over 150 cities worldwide [20], causing widespread problems in both the built environment and infrastructure, resulting in significant economic losses and, in some cases, the loss of human lives. More specifically, the main effects can be summarized as (1) seawater intrusion or protrusion [21–24], (2) linear network damage such as roads, irrigation and electricity networks [25]; and (3) building damage.

The management of this phenomenon is an extremely complex process with an uncertain outcome due to the fact that: (a) the first visible signs of this phenomenon tend to be recorded at times later than its initial activation; (b) it may be difficult to delineate the extent of the affected area since no sign of subsidence may be observed on the ground surface and (c) the failure mechanism is complicated by the interplay of multiple factors, making it hard to determine the extent of its impact.

The assessment of pre-event risk and post-event damage due to land subsidence is highly correlated with ground movement deformations. In terms of detecting and monitoring land subsidence phenomena, there are two prevailing techniques: (a) Geodetic surveys [26–28] and (b) remote sensing techniques. Regarding the former, it necessitates costly equipment and measures deformations on a point-by-point basis. It is mainly used for the accurate measurement of the deformation after the phenomenon activation. During the last two decades, Earth Observation (EO) techniques and technologies have been widely applied in land subsidence. Differential Interferometric Synthetic Aperture Radar (DInSAR) and Global Positioning System (GPS) are the most popular EO techniques with numerous applications around the world [2,3,18]. The outcome of the implementation of the DInSAR technique is based on the analysis of two different radar images gathered over the same area at different times with the same acquisition mode and properties [29].

Using these techniques, one can detect the initiation condition, the spatiotemporal fluctuations, and the extent of the affected area.

Both the activation and consequences of this geohazard are difficult to predict as they depend on factors characterized by major uncertainties, such as an area's geological, geotechnical, and hydrogeological conditions, in addition to the influence of human activities. Numerous studies have been conducted to estimate the correlation between groundwater withdrawal and vertical deformation rates [7,18,30–39]. In general, both the extent and rate of vertical deformation are proportional to the groundwater level drop and the mechanical characteristics of the associated geological formations.

The main objectives of the study are to (a) present significant land subsidence examples in selected areas around the world (USA, Mexico, China, Japan, Indonesia, Iran, Italy, Spain, and Greece), highlighting the increasing intensity of these events; (b) understand the main causal factors driving this process and (c) empathize the valuable information which can be acquired by modern remote sensing techniques for the determination of the spatiotemporal distribution of the subsidence. Besides the fact that land subsidence has caused significant economic losses in the 20th century due to the rising water demands, the determination of the extent to which the primary causal factors contribute to this geohazard is still in its early stages on a global level. The main contribution of our study is the synoptic presentation of several selected papers that describe in detail land subsidence phenomena worldwide in such a manner that readers can independently evaluate the derived information. Our research is among the initial efforts to investigate the causal and triggering factors behind the emergence of this phenomenon. The study of historical subsidence phenomena can help local and regional competent authorities to understand the risks arising from their occurrence. This knowledge will enable them to take appropriate mitigation measures to ensure the future safe development of agricultural, tourism, housing, and other economic activities.

2. Land subsidence in the United States of America (USA)

The USA had the highest growth of any country worldwide during the 20th century. Therefore, the water requirements needed to meet its industrial and agricultural needs, as

well as those of intense urbanization, were enormous. These demands have led to extensive overexploitation of aquifers and the activation of land subsidence. According to data from sites of hydrogeological interest in 1975 [40,41], aquifer overexploitation in eight of the sites exceeded $700 \times 10^6 \text{ m}^3/\text{year}$ (south and southwestern USA), and in 30 of the sites was between 30×10^6 and $700 \times 10^6 \text{ m}^3/\text{year}$ (south, central and western USA).

2.1. Las Vegas, Nevada

Las Vegas Valley is a rapidly growing metropolitan area. The systematic over-pumping of aquifers to meet the needs of the increasing population began in 1950 [42]. The drawdown of the aquifer in the west–north–western section of the valley exceeded 90 m during the early 1990s [43]. This situation, combined with the geo-tectonic characteristics of the area, led to the activation of land subsidence. The recorded vertical displacements in 1948, in parts of the valley, exceeded 2 m compared to data from 1935 [44], causing significant damage to roads, houses and other buildings (Figure 1).

An earlier study, which was carried out using interferometric synthetic aperture radar (InSAR) techniques for the period 1992–1997, found that the maximum vertical deformation rate was around 19 cm [45]. Moreover, it was observed that the spatial extent of the deformations was related to both the geological and tectonic structures (faults) and the thickness of the clay layers. Considering the land subsidence map for the period 1963–2000 [46], the maximum values appear to occur in the north-eastern part of Las Vegas Valley and exceed 170 cm. New studies conducted in the period 2000–2010 [47] found that the land subsidence rate has declined significantly over the last decades due to measures that were taken to reduce aquifer overexploitation, which led to an increase in the groundwater level.



Figure 1. (A) drill pipes lifting, (B) Damaging house in the Windsor Park District due to land subsidence [48].

2.2. San Joaquin Valley, California

The San Joaquin Valley in California is one of the world's largest agricultural areas [49]. Therefore, its water supply demands are a key priority for local authorities. Aquifer overexploitation has led to extensive land subsidence across the valley [25]. An area of 13,000 km² has vertical deformation values of at least 0.3 m [50,51]. Notably, the maximum recorded land subsidence value in this area is almost 9 m [52] (Figure 2).

To address this phenomenon, local authorities conducted surface water inflow projects in the late 1960s, resulting in reduced demand for groundwater. Since the end of 1971, the annual land subsidence rate has been reduced by 50–70%. However, the intense droughts between 1976–1977, 1990–1994, 2007–2010, and 2012–2017 significantly reduced surface water inflow and increased overexploitation of the aquifer. This situation resulted in an

increase in land subsidence rates, reaching values observed before the construction of surface water inflow projects [53,54]. A recent study compared data on groundwater level and vertical land motion and evaluated that 0.5–1.5 years are required for groundwater level in aquitard and aquifer units to equilibrate. However, during this period, residual compaction of aquitards and land subsidence continues beyond the drought period [55].

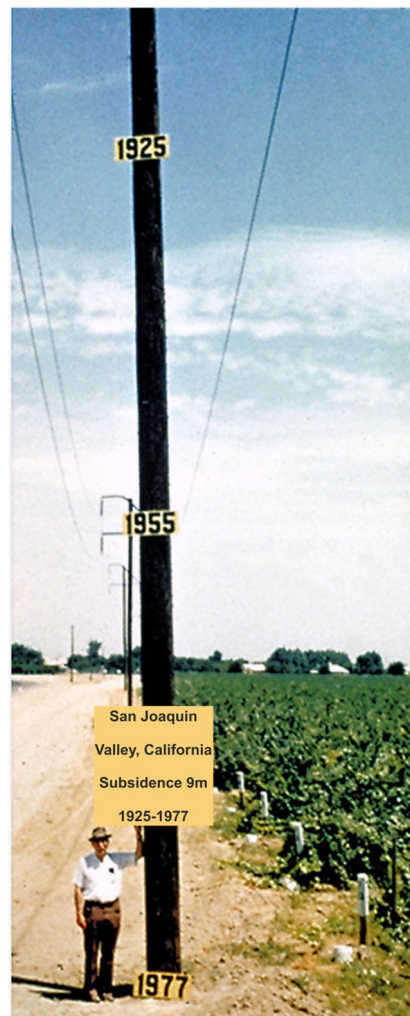


Figure 2. The maximum vertical deformations in the San Joaquin Valley, California. The signs on the column were placed at the approximate former altitudes of the earth's surface between 1925 and 1977 [56].

2.3. Long Beach Area, California

The Long Beach area of California represents the most important example of oil extraction-induced land subsidence. Since the onset of oil extraction in this area in the early 1940s, land subsidence has been observed. The maximum subsidence value was recorded in the Wilmington area and reached 8.8 m [8]. As a result, seawater inundation of inland areas has occurred, causing significant damage (Figure 3). Researchers determined that to deal with this phenomenon, and it was necessary to restore the volume of the extracted oil by injecting water back into the wells. However, this method, despite its high cost, did not yield the expected results.



Figure 3. (A,B) Seawater rushes over the mainland in the Long Beach area, California, (C). Water injections [57].

2.4. Santa Clara Valley, California

The first land subsidence phenomena due to aquifer overexploitation in the United States were recorded in California's Santa Clara Valley [58]. During the first half of the 20th century, agricultural activities intensified. After the Second World War, during the period 1945–1970, rapid population growth changed the local economy from primarily rural-based to industrial and urban. The evolution of land subsidence is closely linked to the primary factors that affect the pumping of groundwater, such as population growth, land use change and surface water inflow [59].

The maximum land subsidence values occurred in San Jose (4 m) between 1910 and 1995. This phenomenon was more intense in the northern part of the valley near the San Francisco Bay area. An area of approximately 44 km² experienced land subsidence in the range of 0.5–2.5 m, resulting in substantially increased flooding risk [60].

An economic study [61] estimated that the direct cost of the land subsidence phenomenon in this area was over \$131.1 million in 1979 and \$332 million in 2003. This amount includes the cost of constructing embankments around the southern part of San Francisco Bay, maintenance of existing embankments, elevation of the railway and road network, increasing the sewage capacity and constructing pumping stations. Notably, approximately 1000 water wells were damaged or destroyed during the period 1960–1965 due to land subsidence.

2.5. The City of Houston, Texas

The largest urban area in the United States affected by land subsidence is the metropolitan city of Houston in Texas. The city was established in 1836 as a commercial city from which steamers transported goods to the southeast. Aquifer exploitation to meet domestic and agricultural needs began in the late 1880s. The opening of the waterway channel in 1914 made Houston one of the largest ports in the United States. The area's industry grew significantly during the Second World War, resulting in an increase in the population. To address the problem of aquifer overexploitation, surface water channels were created in the central and eastern districts of Houston. However, recent urban development towards the north and west of the city continues to be based on aquifer exploitation [59,62].

Based on previous studies, land subsidence exceeding 0.3 m was observed over an area of more than 8000 km² until 1979. The highest deformation values, reaching up to 3 m, occurred in the Pasadena area (Figure 4). After the inflow of surface water in the east of Houston commenced at the end of the 1970s, vertical deformation rates decreased significantly [63]. According to vertical displacement data for the period 1906–1995, the city's intense urbanization appears to have shifted the subsidence phenomenon from the bay to the inland areas to the north and west of Houston [64,65].

The regulations for reducing groundwater withdrawal [66] have been enacted as a result of the need to mitigate vertical displacements. In addition, land subsidence is likely to continue throughout the 21st century [67]. Vertical deformation values exceeding 49 mm/year (using the Advanced Land Observation Satellite) and 34 mm/year (using

the Sentinel-1A/B satellite) were recorded in the periods July 2007 to January 2011 and December 2015 to August 2017, respectively, affecting significant parts of the Houston area [68].



Figure 4. Land subsidence in the area of Pasadena [69].

2.6. Arizona

Land subsidence in central and southern Arizona was first recorded during the 1940s, primarily in rural areas [70]. This subsidence was driven by systematic over pumping of the aquifer, which led to a significant water level drop exceeding 150 m [71,72]. Notably, vertical displacements in this area exceeded 5.7 m both in the western part of Phoenix, near the Air Force Base, between 1957–1991 [73] and in the Eloy region between 1948–1985 [74]. The Arizona Water Resources Department has monitored vertical displacements in this region since 2002 using InSAR techniques and has identified more than 25 areas that have suffered from land subsidence, covering an area exceeding 7300 km² [75]. These have since been expanded to encompass more than 26 individual land subsidence areas, covering an area exceeding 7500 km² [76]. This land subsidence has also led to the formation of extensive surface ruptures (Figure 5). Their size varies and may exceed 3 m in width and 10 m in depth [77]. The Arizona Geological Survey (AZGS) has mapped more than 251 km of surface ruptures since 2007 [78]; this number had exceeded 273 km by 2017. Overall, the current trends in the evolution of vertical displacements and surface ruptures in this area demonstrate that this geohazard is still ongoing and will likely continue into at least the near future.



Figure 5. The effects of land subsidence in the area of Arizona. (A) Max vertical deformation reached 75 cm between 1940–1950 [79]. (B) Surface ruptures were reopened after a major rain in August 2005 [77]. (C) Surface ruptures [80].

3. Land Subsidence in Mexico

In recent decades, urban development in several Mexican cities, combined with intensive agricultural activity, has caused land subsidence [81]. The pumping of the aquifers provided 70% of the water needs of 122.3 million of Mexico's inhabitants in 2013 [82], leading to a significant water level drop and consolidation of compressible subsurface formations [83]. This phenomenon affects a significant part of the country. According to recent research that was conducted using InSAR techniques for the period 2007–2011 [84], 21 different regions were identified as experiencing land subsidence. The phenomenon is more intense in Mexico City, where vertical displacements of over 30 cm/year were recorded, whereas vertical movements in other districts did not exceed 5–10 cm/year. Some examples are as follows.

3.1. Mexico City

Mexico City, with a population of 9 million, is the most important economic, industrial and cultural center of the country. This city is located over alluvial deposits, and land subsidence began to appear in the late 18th century [85]. The groundwater level drop of around 1 m/year has caused vertical displacements of up to 40 cm/year. During the past 100 years, the total vertical displacements in the center of the city reached values of up to 7.5 m [86]. As a result (Figure 6), extensive damages have been identified in urban infrastructure and transportation and drainage networks [87–93]. To address this issue, the local authorities required the use of deeper foundations for major constructions, including the use of piles.



Figure 6. Damage due to land subsidence in Mexico City. (A) Vertical differential deformation [94]. (B,C) Damage to infrastructure [95].

Several surveys have been conducted to determine the evolution and rate of vertical displacements in Mexico City. Initial studies were based on geodetic measurements [96] and piezometers [97,98], whereas more modern research has used GPS [88] and InSAR techniques [36,88,99–105]. The first studies recorded land subsidence of up to 50 cm/year in the historical area and the city center (1940–1960), while later studies (2002–2007) identified lower vertical displacements reaching values up to 30–35 cm/year in the eastern and central parts of the city. The evolution of the phenomenon to date is confirmed by multiple studies conducted using Earth observation techniques or GPS leveling measurements [106–108]. These studies confirm that the vertical displacements between 2014 and 2020 have reached 39 cm/year [109], increasing the number of people living in zones at high to very high risk to 1.5 million.

3.2. The State of Sonora

The state of Sonora is in the northwestern part of Mexico, and since 1960, its aquifer has been overexploited. According to surveys in 1993 [110], the pumping of groundwater was three times larger than the inflow of water into the aquifer due to the low cost of pumping. This has resulted in the salinization of the aquifer, causing significant damage to 8000 hectares of irrigated land.

3.3. Celaya

Celaya is the third-most populated city in Mexico's Guanajuato region, with a population of 300,000 inhabitants (as of 2005). In recent decades, the total pumping of its aquifer has increased gradually; in 1985, pumping occurred at a rate of $538 \times 10^6 \text{ m}^3/\text{year}$; in 2004, it reached $593 \times 10^6 \text{ m}^3/\text{year}$, and in 2008 it approached $600 \times 10^6 \text{ m}^3/\text{year}$ [111]. As a result, the overall groundwater level drop for the period 1956–2008 reached 90 m [112]. Using data from Envisat and InSAR techniques for the period 2003–2006, land subsidence was observed in the center of the city at rates ranging from 2–3 cm/year [113,114] to 7–10 cm/year [115]. During the period 2007–2011 [84], the vertical displacements approached 9 cm/year, while for the period 2012–2014, the average value was 4–6 cm/year [116]. All of the aforementioned land subsidence has caused significant damage to the buildings and infrastructures of this city [117].

3.4. Morelia City

Morelia is the capital and largest city of the Michoacán state in central Mexico. The expansion of the city (by an average of $1.8 \text{ km}^2/\text{year}$ between 1975 and 2020) has led to groundwater overexploitation and triggered land subsidence, causing significant damage to houses and infrastructure [118]. To constrain the patterns and rates of subsidence, this area has been investigated using satellite observations [84,114–116,119,120]. All the studies have consistently found that the maximum vertical displacements are taking place in the northern part of the area. The vertical displacement rates have been estimated at 3.5 cm/year for the period 2003–2006 [114,115] and 7–8 cm/year for the period 2003–2010 (Figure 7) [119,120], 7 cm/year for 2007–2011 [84], 4–6 cm/year for 2012–2014 [116] and 2.74 cm/year for 2014–2017 [121]. Additionally, a recent study that used Earth observation techniques estimated subsidence rates up to 9 cm/year between 2014 and 2021 [122].

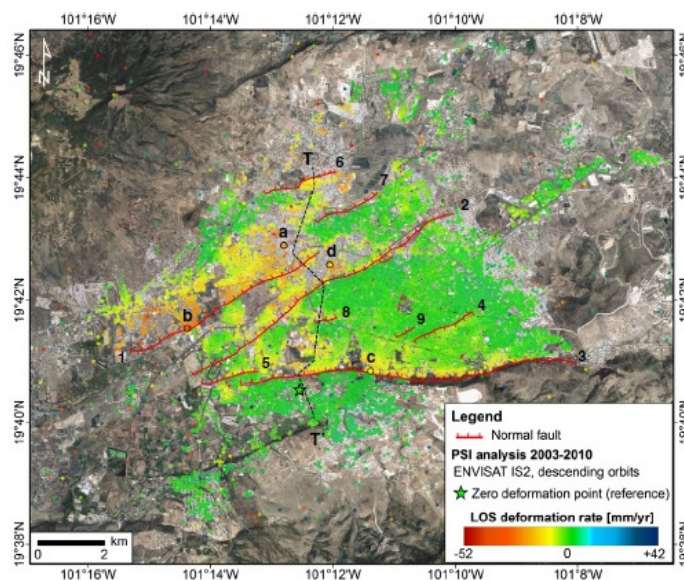


Figure 7. Vertical deformation rate in Morelia between 2003–2010 using PSI analysis of ENVISAT images [119].

3.5. The City of San Luis Potosi

San Luis Potosi is located in north-central Mexico and has also suffered from the land subsidence phenomenon. Specifically, in the cities of San Luis Potosi and Soledad de Graciano Sanchez, land subsidence became visible during the 1990s and caused significant damage to sidewalks and sewer pipes, as well as generating cracks in the walls and roofs of buildings [123].

4. Land Subsidence in China

Since the mid-20th century, China has experienced rapid agricultural and industrial growth. Consequently, the water demands to meet industrial, agricultural and urban needs have increased. Statistical data [124] show that 164 different regions with a total extent of 181,300 km² have been overexploited. The areas with the highest over-pumping levels occupy 77,000 km², i.e., 42.5% of the total overexploited region. According to groundwater monitoring systems in 17 provinces of North China (with a total extent of 750,000 km²), the total groundwater reserves decreased by 15.1 billion m³ between 2001 and 2002. Generally, from 1994 to 2002, the groundwater reserves in North China decreased consistently, with some fluctuations between 1994 and 1998. The largest decreases were recorded in 1997 (17 billion m³) and 2001 (20 billion m³) [125].

Land subsidence due to aquifer level drops had been observed in 90 cities by 2005; of these, 80% are located in areas along the coastal zone [126]. A total area of approximately 70,000 km² is affected by these phenomena [32]. In recent years, the areas with land subsidence greater than 200 mm increased from 79,000 km² in 2009 to 90,000 km² in 2012 [127].

As noted above, this phenomenon is located both along the coastal urban area [127–132] and within urban cities such as Shanghai [128,133,134], Tianjin [135–137], Taiyuan [138], Suzhou [139,140], Cangzhou [141] and Beijing [142], as well as in cities located within the Delta of Yangtze Suzhou River such as Wuxi and Changzhou [143]. Some examples of this phenomenon are as follows.

4.1. Shanghai

China's largest city, with a population of 24 million, is located on the estuary of the Yangtze River. The aquifer, which occurs within Quaternary deposits, has a thickness ranging from 200 to 300 m. According to historical data, groundwater pumping first took place in 1860, with the first subsidence recorded in 1921 [134]. The exploitation of the aquifer continued, reaching 2 m³/s in 1962, and, as a result, the rates of vertical displacement increased. By 2005, the average vertical displacements in the urban area reached 1.92 m, while the maximum values were as high as 2.9 m [134].

In terms of planning, the latest regulations for managing land subsidence in Shanghai were approved in 2013. Relying on these regulations, land subsidence across the entire administrative region has been reduced to around 5 mm per year [144]. However, vertical displacements of up to 26 mm/year were observed in the districts of Fengxian, southern Jinshan and Songjiang for the period between January 2018 and March 2020 [145], thus highlighting that the area is still subsidence-prone, causing significant problems in the city.

4.2. The Cities of Suzhou City, Wuxi City and Changzhou City

These cities are located southwest of Shanghai along the Yangtze River. They overlie Quaternary deposits with a thickness of 150–220 m that thicken from the west to the east and from the south to the north [139]. The first land subsidence phenomena were observed in this area in the 1960s. In recent decades, the total area with a vertical deformation exceeding 20 cm approached 6000 km². The maximum subsidence values of 84.2 cm have been recorded in Jiaxin City [146].

4.3. Beijing

Beijing is the capital of China and the second-largest city in terms of population (14.5 million). Two-thirds of its drinking water and its industrial water supply are both derived from its aquifer, with the annual water pumping volume exceeding 25×10^8 m³ [142]. The first land subsidence was recorded in 1935 [126]. Concurrent with the industrial development of the city to the east in the period 1955–1983, the vertical displacements increased to rates of 16–28 mm/year [147]. Measures taken by the government between the 1980s and 1990s succeed in mitigating this phenomenon. However, since 1999, the combination of prolonged drought and rising water demand has led to re-overexploitation

of the aquifer and reactivation of the subsidence phenomenon. As a result, the average vertical displacements rates during 1999–2009 were 15–25 mm/year, with the highest value observed in 2009 (137 mm/year).

The maximum land subsidence rate during the period 1935–2009 reached 1163 mm [148] and 1980 mm over the past three decades (1992–2022) [149]. According to data collected in 2012 [147], two-thirds of the Beijing plain was affected by land subsidence. An area of 2996 km² experienced total vertical displacements exceeding 10 mm; in addition, an area of 1538 km² experienced total land subsidence exceeding 30 mm and an area of 50 km² experienced total vertical displacements exceeding 500 mm [150].

The South-to-North Water Diversion Project (which was created in 2015) significantly changed the area's land subsidence trends. Specifically, two years after the outset of this project, the area with land subsidence decreased from 79% to 60%, while the maximum vertical displacement rate decreased from 141 mm/year [151] to 135 mm/year [152].

4.4. Tianjin City

Tianjin city is a major industrial city located along the Bohai coast to the west of the Pacific Ocean with a population of 7.5 million. This city overlies Quaternary deposits with a thickness varying from 100 to 330 m in the north and from 300 to 430 m in the south of the area [136]. The first recorded land subsidence was in 1923 [126] and resulted from the combined effect of the aquifer level drop and the area's tectonic structure. The phenomenon intensified during the period 1966–1985 when the volume of pumped water reached 1×10^8 m³/year [131]. The average vertical displacement rate in this city was 26 mm/year for the period 2011–2012. The area with land subsidence greater than or equal to 10 mm in 2013 occupied 7838 km². In addition, the extent of land subsidence with values greater than or equal to 50 mm was close to 1637 km² [127], and the area in which the vertical displacements exceeded 50 cm reached 7270 km² [150,153]. The maximum recorded vertical displacement values in this area exceed 3.1 m [20,126]. Thus, given the area's location and low elevation, the ground surface is below sea level in the coastal zones, resulting in significant damage to infrastructure. Numerous pump stations have been constructed to prevent the intrusion of seawater within the urban area (Figure 8).

Recent studies have highlighted that the subsidence rate has increased significantly over time. In detail, the average vertical displacement rate has increased from 2.4 cm/year for the period 2010–2014 to around 5 cm/for the period 2015–2019 [154,155].



Figure 8. Land subsidence in the area of Tianjin city. (A) An increase in the height of the embankments due to land subsidence 1995 and 1998 1998 Governance Section. (B) Damage to the water supply system [156].

4.5. Hebei Province

Hebei Province is located to the west of Bohai Bay (Yellow Sea), and its population is 71 million. This area is founded on Quaternary formations with thicknesses varying

from 300 to 580 m [157]. The first land subsidence deformation was recorded in Handan in 1960, and in recent decades, the phenomenon has expanded to affect an area of 70,000 km², equivalent to 97% of the province. The total area for the year 2013, in which vertical displacements were greater than or equal to 50 mm, was close to 11,400 km² [127]. In addition, land subsidence exceeding 50 cm affects an area of 6430 km² [150]. During the 1990s, an area of 337.9 km² was identified in which the vertical displacements were more than 1 m [153]. The largest subsidence values for the period 1970–2013 reached 2.68 m and were recorded in Cangzhou. In addition to land subsidence, surface ruptures have also been observed in the Hebei Province: according to recorded data, 228 surface ruptures were detected in 1989, 402 in 1993, 482 in 2000, and 839 in 2013 [158].

4.6. The City of Shian

The city of Shian is built on the southern part of the Lóane plain and has a population of almost 8.5 million. It is located on Quaternary formations whose thickness varies from 300 to 1000 m [159]. The first land subsidence phenomena were recorded in the late 1950s, while surface ruptures occurred after 1976. The major M_W 7.6 earthquake on 28th July 1976 resulted in an increase in the number of surface ruptures [139,160].

5. Japan

The rapid concentration of population in the urban centers of Asian coastal cities has resulted in the overexploitation of aquifers and caused significant problems, such as land subsidence and water salination [161,162]. This phenomenon is particularly intense in Japan's major cities such as Tokyo [163], Osaka and Nagoya, where land subsidence was observed in the period 1950–1970 [164]. A few representative examples are as follows.

5.1. Kanto–Tokyo Plain

The Kanto Plain is located in central Japan and covers an area of approximately 16,000 km². Tokyo city, with a population of 13.1 million people (2011), is the largest urban area in Japan and is located in the southern part of the plain. Tokyo's first water supply system was established in 1913 [165]; subsequently, numerous wells have been drilled to meet the city's needs. Pumping activities increased dramatically during the economic growth of the 1950s and 1960s; for example, pumping in the eastern part of the city increased to 1 million m³/day [166]. However, over-pumping of the aquifer has caused severe land subsidence. The maximum values reached 23.89 cm/yr in 1968 in the area of Edogawaw-Ku [167]. To reduce the impacts of this phenomenon, the Japanese government established rigorous laws in 1957, and, as a result, pumping in eastern Tokyo decreased from 800 mm/year in 1960 to 100 mm/year in 1980 [168].

5.2. Nobi Plain

The Nobi Plain is located in central Japan and occupies an area of approximately 1800 km². It is one of the country's most densely populated areas, with 1000 inhabitants/km² [169]. In the 1920s, the groundwater level was close to the surface [170]. However, since 1945, there has been a dramatic increase in the pumping of the aquifer to meet industrial and agricultural needs. This situation led to groundwater drawdown and the onset of land subsidence. This phenomenon increased exponentially in the following years, with vertical displacements exceeding 20 cm recorded in 1973 [171].

Strict pumping regulations that were introduced successfully mitigated the negative consequences of this phenomenon—the area in which the rates of vertical displacement exceeded 1 cm decreased from 283 km² in 1975 to 9 km² in 2004 [172]. In addition, the earth's surface in some places, such as Gocho and Matsunaka, in the east–southeast of the plain, was uplifted by 20–25 mm [172].

6. Indonesia

Many Indonesian cities, such as Jakarta, Bandung, and Semarang, have been affected by land subsidence due to aquifer overexploitation. This phenomenon has caused extensive damage to buildings and infrastructure and flooding in coastal areas.

6.1. The City of Jakarta

Jakarta, the Indonesian capital, has a population approaching 8.7 million people (2004) and requires large volumes of water to meet its urban and industrial needs. This situation has resulted in aquifer overexploitation and the onset of land subsidence [26,173,174]. According to GPS measurements and InSAR techniques, for the period 1982–2011, vertical displacements ranging from 1 to 15 cm/year were widely observed, with some higher values reaching 20 to 28 cm/year [175]. The maximum land subsidence values are observed mainly in the coastal area, which exceeded 4.1 m during the period 1974–2010 (Figure 9). The ongoing subsidence trend in the coastal area is confirmed by a recent study that identified vertical displacement rates of around 30 to 40 mm/year between March 2017 and April 2020 [176].

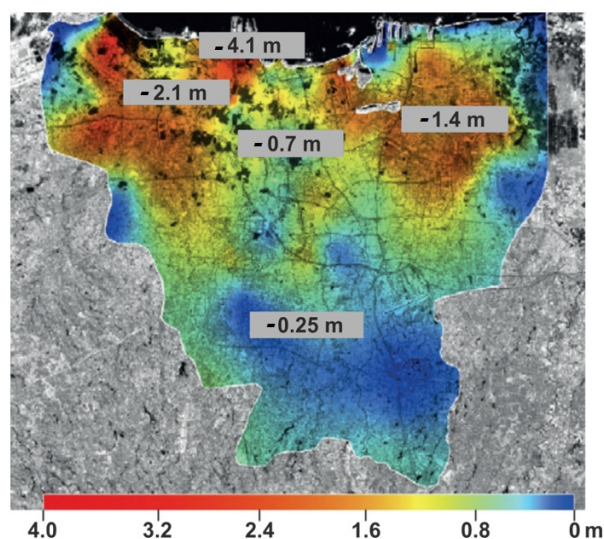


Figure 9. Land subsidence due to the overexploitation of the aquifer between 1974–2010 in Jakarta, Indonesia [177].

6.2. Semarang

Semarang is a city that covers approximately 373.7 km² and is located in the northern part of the province of Java, with a population approaching 1.5 million inhabitants (2010). In this city, during the early 1990s, intense urbanization occurred, particularly in the northern coastal zones [178]. Large volumes of groundwater were pumped to cover the needs of the population, industry and commercial activities [178]; specifically, the total volume of pumped groundwater increased from 23 million m³ in 1990 to 38 million m³ in 2000 [179]. However, this systematic overexploitation caused severe land subsidence phenomena [23,180], which have become gradually larger over time [181]. The vertical displacements, according to InSAR data, varied from 8 cm/year during 2007–2009 [179] to around 15 cm/year (in specific areas) during 2015–2017 [182]. In the case of coastal cities such as Jakarta and Semarang (Figure 10), land subsidence also leads to the phenomenon of severe flooding [23].



Figure 10. (A) Floods due to the land subsidence phenomena in Jakarta [183], (B) Coastal flooding on April 2009 in Semarang [23].

6.3. Bandung

Bandung, the capital of the Java province, has a population of 2.4 million inhabitants. In this area of Indonesia, land subsidence has been observed due to groundwater overexploitation [184–186]. Studies conducted between 2000 and 2011 indicate that this area has suffered from vertical deformations with an average annual rate of 8 cm/year [175]. These values have since increased to 10–12 cm/year for the period 2015–2017 [187].

7. Iran

In Iran, land subsidence due to aquifer over-pumping of the aquifer has been observed in the cities of Tehran, Mashhad, Kashmar, Varamin, Kashan and Rafsanjan [188]. Tehran, with a population of 9.1 million, is the capital of Iran; the average altitude of the city is 1191 m, while the Tehran basin occupies an area of 2250 km². This area has undergone intense urbanization in addition to significant agricultural and industrial activities, resulting in large water needs. Systematic aquifer overexploitation has led to significant groundwater level drops; between 1984 and 1991, the level drop reached 4 m, from 1995 to 2004, it was 6 m, and for the period 2007–2012, a further 1.65 m water drop occurred. Notably, small periodic variations in aquifer level were observed during the years 1991–1995 and 2005–2006. Therefore, the overall water level drop for the period of 28 years was 11.65 m, i.e., 42 cm/year [189]. This aquifer overexploitation has also resulted in land subsidence, with the first vertical displacements recorded in 1990 [190]. The maximum values recorded in 2004–2008 exceeded 200 mm/year [191], while the cumulative vertical displacements reached 39.6 cm in 2004–2010 and 88.4 cm in 2014–2017 [192]. These high subsidence rates have caused damage to settlements, roads and infrastructure (Figure 11).



Figure 11. Damages due to the overexploitation of the aquifer in Tehran: (A) uplifting of boreholes (Sabashahr). (B) damage to the electricity network red arrows showing the deviation from the vertical (Sabashahr). (C) Damaged boreholes suggesting a drop of 30 cm (Eslamshahr and Ahmadabad) [193].

8. Italy

8.1. Venice

The phenomenon of land subsidence in the Venice region is more complex than in the other examples discussed so far. In addition to land subsidence induced by the groundwater level drop, the sea level in the Venetian Lagoon has increased due to climate change. During the past century, the vertical displacements relative to sea level reached 23 cm. Of this value, 12 cm can be attributed to land subsidence due to natural (3 cm) or anthropogenic (9 cm) causes, while 11 cm can be attributed to sea level rise [194]. The resulting increase in flooding has led to both direct and indirect damage, causing significant concern to local authorities. Overpumping of the aquifer in this area is related to the creation of the first industrial plants in the 1930s, with the maximum over-pumping rates recorded in the period 1950–1970. This scenario resulted in land subsidence along the Marghera industrial zone (7 mm/year), the southern part of the lagoon (6 mm/year), the city of Venice (5 mm/year) and the northeast border area of the lagoon (2 mm/year) during the period 1952–1968. The highest values were measured between 1968 and 1969 in the Marghera industrial zone (17 mm) and the city of Venice (14 mm) [195]. Local authorities implemented measures to reduce industrial overexploitation of the aquifer in 1970; these measures resulted in the rapid recovery of the aquifer and an increase in its groundwater level. As confirmed by measurements, the phenomenon of land subsidence was eliminated in 1973 [196,197]. Taking into account measurements that were acquired between 1973 and 1993, the stability of the inland area was confirmed, however, decreases of 1–2 mm/year along the coastline and in the north and south areas of the city were recorded [198–200]. Given that the Adriatic Sea level increased by 1.23 ± 0.13 mm/year from 1872 to 2019 (after removing the effects of subsidence) [201], Venice city continues to face the joint problem of land subsidence taking place at the ends of the lagoon combined with rising sea level due to climate change.

8.2. Ravenna

The Ravenna area is in northern Italy in the south-eastern part of the Padou river and covers an area of approximately 38,000 km². Over the last century, extensive land subsidence has been recorded in this area due to both natural and anthropogenic factors. From 1897 to the Second World War, the average vertical displacement rate was 5 mm/year. After the Second World War, intense industrial growth combined with the extraction of natural gas led to the overexploitation of the aquifer. This situation has resulted in a significant increase in vertical displacement values, with values reaching 110 mm/year recorded in 1972–1973 [202,203]. To combat this issue, the state took strict measures, and the phenomenon was reduced. Notably, the overall vertical deformation for an area covering around a third of Ravenna (including the city and a significant part of the coastal zone) is close to 1 m. In an area covering 10 km² between the historic center and the coastline, the maximum subsidence values exceed 1.6 m. In recent decades, the subsidence phenomenon in the mainland has significantly decreased; however, some coastal areas continue to subside at a rate of around 10 mm/year [204].

8.3. Bologna Region

During recent decades, significant land subsidence has been observed in the Bologna region. This city is situated on Holocene and Middle Pleistocene deposits with a total thickness of 400 m. Considering previous research that was conducted for the period 1974–1981, the vertical deformation rate due to the overexploitation of the aquifer exceeded 11 cm/year. According to recent studies [205], this rate (due to policy changes) appears to exhibit a consistently decreasing trend with seasonal variations.

9. Spain

In Spain, intensive overexploitation affected 77 aquifers [86], most of which are located in the southeast of the country. The water needs for Spain's agriculture and tourism are

rising in the summer months when water availability is lower and, in general, the demand exceeds the available water supply [206]. A typical example of this situation is the city of Murcia, which is located on the bank of the Segura River in south-eastern Spain. In this area, aquifer over pumping has caused severe land subsidence, damaging both infrastructure and city buildings. According to a previous study [207] using satellite systems (TerraSAR-X), for the period between July 2008 and September 2009, a subsidence rate of 5 mm/year was observed in this area, with maximum recorded subsidence values of 35 mm/year.

10. Greece

10.1. Kalochoi, Thessaloniki

In the village of Kalochoi [1,2,208–211], rapid industrial development in the early 1960s, combined with extensive aquifer over-pumping by the Water Company of Thessaloniki, led to a significant water level drop in the aquifer which, over time, has reached a magnitude of 40 m [210,212]. Researchers suggest that aquifer drawdown has resulted in the consolidation of the underlying alluvial deposits in this area and the onset of land subsidence. The vertical displacements recorded over the last 50 years have reached 3 to 4 m [1]. The maximum recorded deformation occurs in areas where the thickness values of the Quaternary deposits are higher, highlighting the important role of the thickness of these formations in determining their geotechnical behavior [2]. Notably, due to the smooth stratification in this area, no surface ruptures have been observed. However, this phenomenon has caused significant damage in the form of seawater intrusion—currently, the inland areas are located 4 m below sea level, and embankments have been built to protect the village from flooding.

10.2. Anthemounda Valley, Thessaloniki

In Anthemounda Valley [4], the increase in water pumping to meet urban, tourist and industrial needs has led to the consolidation of Neogene and Quaternary deposits and the onset of land subsidence. Due to the area's tectonic structure, subsidence has been observed along the coastal zone of the basin in the Peraia area, causing damage to various houses [213]. Similar phenomena have also been recorded in the vicinity of Thessaloniki International Airport. The correlation between decreasing groundwater levels and vertical deformation has been confirmed by recent studies conducted using InSAR satellite technology [2,4]. More specifically, between April 1995 and June 2001, small displacement rates were observed in the coastal zone of the Peraia settlement, with average values ranging from -1.5 to $+1.5$ mm/year. In contrast, deformation rates recorded in Ano Peraia were much larger, ranging from -10 to -15 mm/year. Recent studies based on Sentinel-1 data (during the years 2015–2019) indicate that vertical displacements are still ongoing throughout the entire basin [214].

10.3. East Larisa Plain

In East Larisa Plain [215–219], systematic aquifer overexploitation to meet agricultural needs has led to a significant groundwater level drop of 50 m over a 20-year period (1981–2001) [220] and the onset of land subsidence since 1986. The occurrence of this phenomenon in areas where the thickness of the alluvial deposits varies significantly (both in the margins and the central part of the plain) has resulted in the formation of surface ruptures. The subsidence phenomenon has also caused considerable damage to villages, farmland and roads. According to a recent InSAR-based study [218], the area exhibits both uplift and subsidence processes with annual rates of up to -2.9 and 6.6 mm/year, respectively, for the years 1995–2008. While some of these changes can be attributed to tectonic movements, there is also a continuous deformation mechanism that correlates strongly with recorded groundwater level changes in this area.

10.4. West Larisa Plain

In West Larisa Plain, the combination of the presence of alluvial formations and aquifer drawdown has resulted in extensive land subsidence that has been observed since 1980 [221]. This phenomenon, due to the area's tectonic structure (presence of active faults), has caused surface ruptures that have damaged the settlements of Farsala and Stavros.

10.5. Thriasio Basin

In the Thriasio basin, which is located 25 km west of the capital of Greece, systematic overexploitation of the aquifer during recent decades to meet the agricultural, industrial and urban needs has led to a significant groundwater level drop and the onset of land subsidence. According to a recent study [222] based on the Persistent Scatter Interferometry (PSI) technique, vertical displacement ranging from -3 mm/year to -10 mm/year was observed for the period between May 1992 and November 2003. These rates reached -3.5 to -5 mm/year (based on Interferometric Point Target Analysis) for the period 2002–2010 [223].

10.6. Amyntaio Basin

In the Amyntaio basin, the systematic over-pumping of the aquifer during the last decades, from both the Amyntaio open pit coalmine (to protect the slopes of the mine) and the wells for irrigation purposes, led to a significant drop level of the aquifer which reaches 70 m [224–226]. This drawdown has resulted in the consolidation of Quaternary deposits and the occurrence of land subsidence and surface ruptures damaging villages and infrastructure (Figure 12). The highest values of vertical displacements, which reached 1.5 m, were observed in areas near the mine. It is worth mentioning that the phenomena were so intense that it was necessary to relocate the settlement of Anargiroi.



Figure 12. (A) Wall fence damaged due to vertical displacements of up to 30 cm at Valtонера village. (B) Damaged building wall and (C) greenhouse at Anargiroi village.

11. Discussion

Land subsidence caused by aquifer overexploitation is a widespread geohazard that has affected significant areas around the world since the early 20th century [227]. The failure mechanism of this phenomenon is complex and depends on the combined action of multiple factors, geological, hydro-geological, morphological, and tectonic settings, and human activities, whereas its intensity is strongly related to aquifer level drops [228–230]. Thus, to manage the risk arising from this phenomenon, it is necessary to understand the geological and tectonic structure of the research area and the geotechnical characteristics of its underlying formations, as well as the impact of anthropogenic activities. The objective of the review paper was to present significant cases of land subsidence due to aquifer exploitation to identify factors that contribute significantly to the occurrence and evolution of the phenomena. In contrast to most review studies, our paper presents the screened papers in sufficient detail so that the reader can derive as much information as possible about the manifestation and evolution of the land subsidence phenomenon in the research

area. This allows the independent evaluation of the relevant papers also from the side of the reader. Table 1 summarizes the present cases with details concerning the cause of overexploitation, and the resulting vertical displacements, whereas Figure 13 illustrates the distribution of the data.

Table 1. Characteristic examples of land subsidence due to aquifer overexploitation worldwide since the early 20th century.

Area	Cause of Overexploitation	Max Vertical Displacements (m)	Vertical Displacements Using Earth Observation Techniques (mm/Year)	Period of Monitoring	Data and Methods
Las Vegas, Nevada, USA	urbanization	>2 [44]	190 [45]	1935–1924 1992–1997	InSAR
San Joaquin Valley, California, USA	agricultural needs	9 [52]		1925–1977	
Long beach area, California, USA	oil extraction	8.8 [8]			
Santa Clara Valley, California, USA	agricultural and industrial needs	4 [60]		1910–1995	
The city of Houston, Texas, USA	agricultural and domestic needs	0.3 [63]	49 [68] 34 [68]	until 1979 2007–2011 2015–2017	ALOS Sentinel-1A/B satellite
Arizona, USA	agricultural needs	5.7 [73,74] 7.5 [86]		1957–1991	
Mexico City, Mexico	urbanization		500 [96] 300–350 [100–105] 390 [109]	1900–2002 1940–1960 2002–2007 2014–2020	Geodetic surveys InSAR Earth Observations techniques and GPS leveling
Celaya, Mexico	agricultural and industrial needs		70–100 [115] 90 [84] 40–60 [116]	2003–2006 2007–2011 2012–2014	Envisat and InSAR techniques ALOS InSAR timeseries Envisat and InSAR techniques
Morelia city, Mexico	urbanization		70–80 [114,115] 70 [84] 90 [122]	2003–2010 2007–2011 2014–2021	InSAR ALOS InSAR timeseries Earth observation techniques
Shanghai, China	urban and industrial needs	2.9 [134]	26 [145]	1962–2005 2018–2020	InSAR timeseries
Jiaxin City, China	agricultural needs	0.84 [146]		by 2002	
Beijing, China	urban and industrial needs	1.16 [148] 1.98 [149]	16–28 [147] 15–25 (max:137) [147]	1935–2009 1992–2022 1955–1983 1999–2009	InSAR
Tianjin City, China	industrial needs	3.1 [20,126]	26 [127] 24 [154,155] 50 [154,155]	2011–2012 2010–2014 2015–2019	InSAR and GPS leveling InSAR and GPS leveling InSAR and GPS leveling
Hebei province, China	urban and industrial needs	2.68 [153]		1970–2013	
Kanto- Tokyo plain, Japan	urban and industrial needs		239 [167]	1968	
Nobi, Plain, Japan	Industrial and agricultural needs	0.2 [171]		by 1973	
Jakarta, Indonesia	urban and industrial needs		10–150 (max: 200–280) [175] 30–40 [176]	1982–2011 2017–2020	InSAR and GPS leveling INSAR (Sentinel-1 SAR data)

Table 1. Cont.

Area	Cause of Overexploitation	Max Vertical Displacements (m)	Vertical Displacements Using Earth Observation Techniques (mm/Year)	Period of Monitoring	Data and Methods
Semarang, Indonesia	urbanization		80 [179]	2007–2009	ALOS-PALSAR satellite SAR interferometry SBAS DInSAR analyses using Envisat-ASAR, ALOS-PALSAR, and Sentinel-1A SAR
			150 [182]	2015–2017	
Bandung, Indonesia	urbanization		80 [175]	2000–2011	InSAR and GPS leveling Sentinel-1/2 and ALOS-2 satellite images
			100–120 [187]	2015–2017	
Tehran, Iran	urban, agricultural, and industrial needs	0.88 [192]	200 [191]	2014–2017 2004–2008	PS-InSAR PS
Venice, Italy	industrial needs		5 [194] 14 [195] 1–2 [198–200]	1952–1968 1968–1969 1973–1993	Geodetic and InSAR Geodetic and InSAR
Ravenna, Italy	natural and man-made factors	1.6 [204]	110 [202,203]	1897–2002 1972–1973	GPS leveling
Murcia, Spain	tourism and agricultural needs		5 (max: 35) [207]	2008–2009	satellite systems (TerraSAR-X)
Kalochori, Greece	industrial needs	4 [1]			
Anthemounda valley, Greece	industrial needs		10–15 [2,4]	1995–2001	InSAR
East Larisa Plain, Greece	agricultural needs		2.9 [218]	1995–2008	InSAR/field observations
Thriasio basin, Greece	agricultural needs		3.5–5 [223]	2002–2010	GPS leveling/field observation

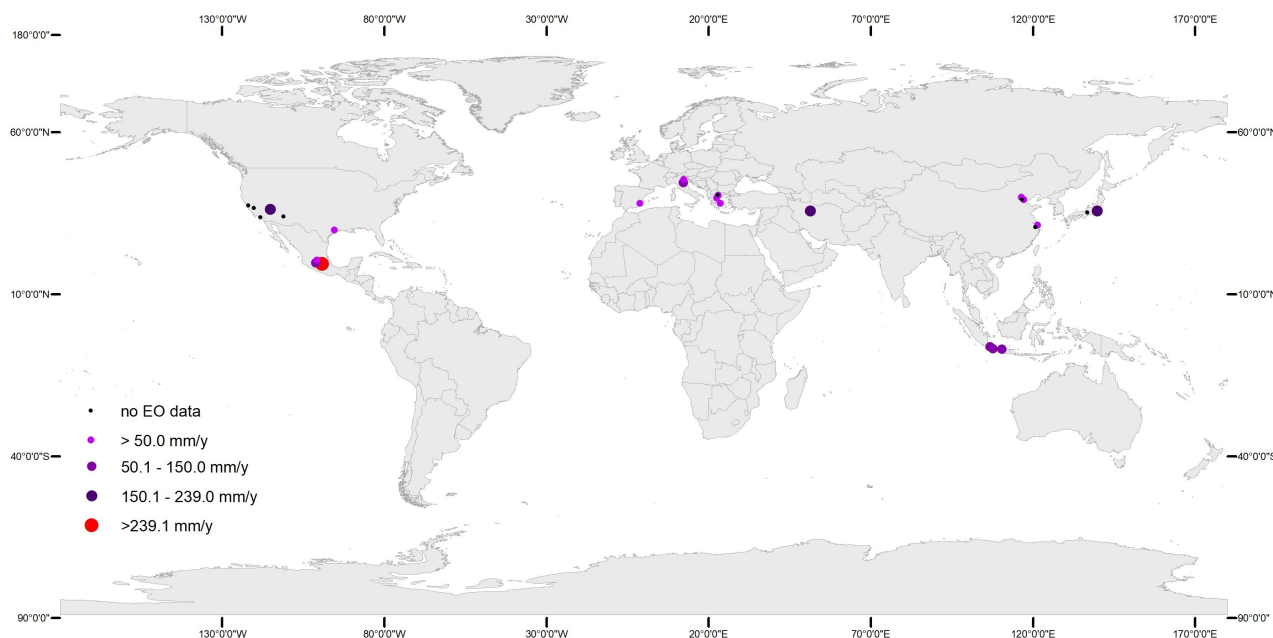


Figure 13. Geographic distribution of the data (Vertical displacements using Earth Observation techniques (mm/year)).

For most of the presented cases, land subsidence phenomena occur mainly in flat areas where unconsolidated sediments accumulate in alluvial basins or coastal plains and in urban or agricultural areas characterized by prolonged dry periods. In addition to the water resource requirements of industry, agricultural needs are particularly high and participate to a large extent in the overexploitation of aquifers. Over 48% of the studied cases concern

land subsidence phenomena induced by groundwater extraction for industrial needs and over 40% for agricultural demands. Oil extraction and mining activities are also responsible for severe land subsidence phenomena that may affect a large portion of settlements, such as the cases in Long Beach in California, USA and Amyntaio plain, Greece [8,224–226]. Furthermore, land subsidence evolves in water-stressed basins, resulting in groundwater depletion and compaction of susceptible aquifer systems. From the present study, it has been derived that maximum recorded deformation occurs in areas with considerable thickness in alluvial deposits, which highlights the important role of the thickness of these formations in determining their geotechnical behavior [2,224–226]. Most of the observed land subsidence occurs in highly populated areas. Characteristic examples are Shanghai and Beijing in China [145,147] and Mexico City in Mexico [96,102,109], which have a long history of land subsidence phenomena induced by over-pumping and dewatering processes because of increased domestic water demand. According to Herrera et al. [231], about 22% of the world's major cities are in areas characterized as potential subsidence areas. Figure 14 illustrates the global spatial distribution of annual groundwater withdrawal (km^3/yr) and the percentage of areas equipped for irrigation with groundwater. Those areas that heavily depend on groundwater resources are areas with high numbers of land subsidence occurrences. Therefore, those areas might be potential areas of land subsidence in the future.

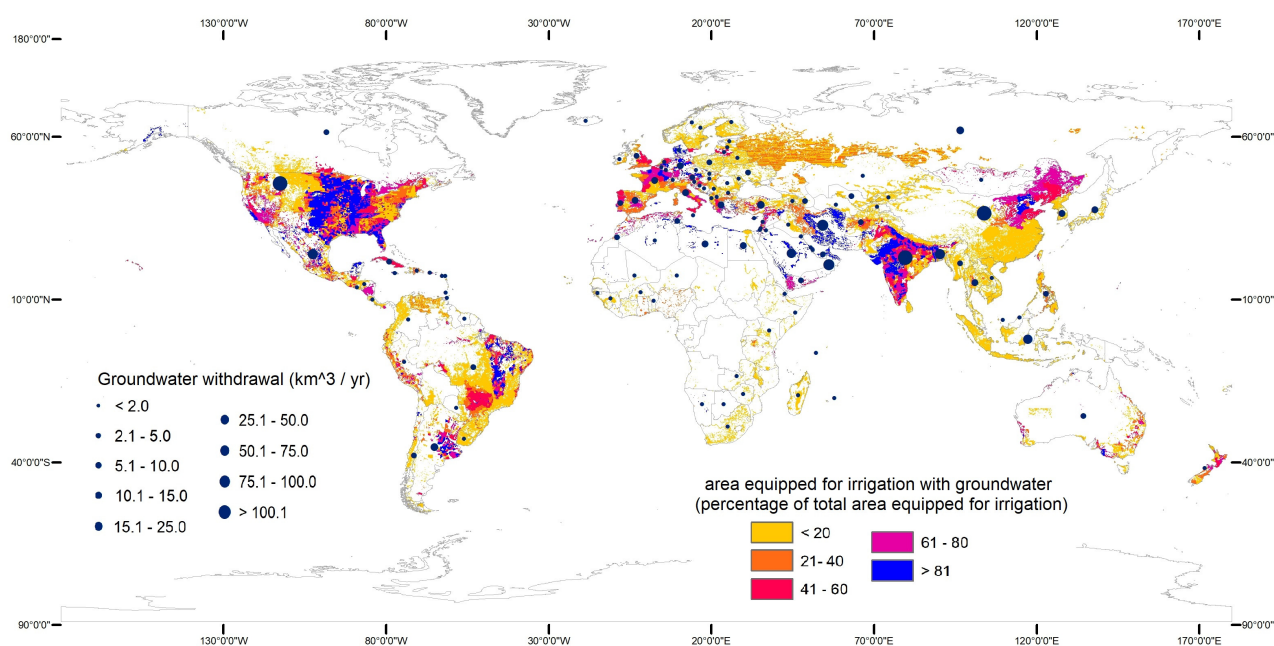


Figure 14. Groundwater withdrawal and an area equipped for irrigation with groundwater (data source [232]).

Another point that should be highlighted is the fact that in coastal areas that are subject to land subsidence phenomena, the sea level rise may enhance the negative effects of land subsidence in the man-made and natural environment. Jakarta and Semarang in Indonesia, Venice and Ravenna in Italy, and Shanghai in China are cases where the sea level rise has a significant contribution to the recorded damages [23,145,201–203]. In most cases, the establishment of optimized aquifer exploitation plans and strict regulations had a positive effect on the displacement rate, with a significant decrease in land subsidence phenomena in Shanghai and Beijing (China), Kanto and Nobi (Japan), Ravenna and Bologna region (Italy) [144,151,152,168,172,202,203,205]. In other cases, aquifer exploitation plans fail, resulting in the continuation of the phenomena, proving in practice the complexity of the mechanism responsible for the occurrence and evolution of land subsidence [145,201,204]. Field investigations (geological, topographic, geodetic surveys, and global positioning system) were

the main investigation tool until the 90s [2,4,45,68,84,114,115,145,149,176,182,187,191,207], whereas remote sensing techniques were the main tool afterward [233–235]. According to Ciampalini et al. [236], traditional ground-based monitoring methods are time-consuming, labor-intensive, and costly, whereas remotely-sensed techniques are more efficient and powerful. Satellite and radar measurements that are obtained from remote sensing techniques prove to be highly accurate, with near-real-time tracking and millimeter accuracy. From our analysis, it was concluded that many studies involve the usage of both geodetic and remote sensing techniques [109,127,154,155,175,194,195,218].

12. Concluding Remarks

The first visible signs of this phenomenon tend to be recorded at times later than its initial activation, thus making the management of land subsidence phenomena a difficult, if not irreversible, situation. In addition, it may be difficult to delineate the extent of the affected area since no sign of subsidence may be observed on the ground surface. The existence of these disadvantages makes the management of this phenomenon an extremely complex process with an uncertain outcome in the context of a future safe development plan. However, despite these issues, modern remote sensing techniques can provide valuable information about the spatiotemporal distribution of the subsidence phenomenon and can help to address these disadvantages. For this reason, it is vital to monitor areas that may be affected by land subsidence using these techniques before further development of agricultural, tourist, residential, industrial or any other socio-economic activities. By adopting this approach, the vertical displacements caused by the overexploitation of the underlying aquifer will be immediately noticed, allowing government and regional agencies to take all the necessary mitigation measures to ensure the safe and sustainable development of society and the environment. In our study, despite the review of several papers that constitute some of the most well-documented work about land subsidence, an additional number of studies could be added to cover different areas around the world. Cases from Africa, North America and Oceania are not included in the present study. Future efforts could involve analyzing a greater number of areas affected by land subsidence phenomena and establishing a closer look at the hidden relations between groundwater fluctuations, displacement rates and geo-environmental settings.

Author Contributions: Conceptualization, P.T. (Ploutarchos Tzampoglou) and P.T. (Paraskevas Tsangaratos); methodology, P.T. (Ploutarchos Tzampoglou) and W.C.; writing—original draft preparation, P.T. (Ploutarchos Tzampoglou); writing—review and editing, I.I., K.K., P.T. (Paraskevas Tsangaratos), X.Z. and W.C.; supervision, P.T. (Paraskevas Tsangaratos); All authors have read and agreed to the published version of the manuscript.

Funding: This research received no external funding.

Data Availability Statement: Not applicable.

Conflicts of Interest: The author declares no conflict of interest.

References

1. Loupasakis, C.; Rozos, D. Finite-element simulation of land subsidence induced by water pumping in Kalochori village, Greece. *Q. J. Eng. Geol. Hydrogeol.* **2009**, *42*, 369–382. [[CrossRef](#)]
2. Raspini, F.; Loupasakis, C.; Rozos, D.; Adam, N.; Moretti, S. Ground subsidence phenomena in the Delta municipality region (Northern Greece): Geotechnical modeling and validation with Persistent Scatterer Interferometry. *Int. J. Appl. Earth Obs. Geoinf.* **2014**, *28*, 78–89. [[CrossRef](#)]
3. Ilija, I.; Loupasakis, C.; Tsangaratos, P. Assessing ground subsidence phenomena with Persistent Scatterer Interferometry data in Western Thessaly, Greece. In Proceedings of the 14th International Congress of the Geological Society of Greece, Thessaloniki, Greece, 25–27 May 2016.
4. Raspini, F.; Bianchini, S.; Moretti, S.; Loupasakis, C.; Rozos, D.; Duro, J.; Garcia, M. Advanced interpretation of interferometric SAR data to detect, monitor and model ground subsidence: Outcomes from the ESA-GMES TerraFirma project. *Nat. Hazards* **2016**, *83*, 155–181. [[CrossRef](#)]

5. Rothenburg, L.; Obah, A.; El Baruni, S. Horizontal Ground Movements due to Water Abstraction and Formation of Earth Fissures. International Association of Hydrological. In Proceedings of the Fifth International Symposium on Land Subsidence, The Hague, The Netherlands, 16–20 October 1995; pp. 239–249.
6. Tzampoglou, P.; Loupasakis, C. New data regarding the ground water level changes at the Amyntaio basin-Florina Prefecture, Greece. *Bull. Geol. Soc. Greece* **2016**, *50*, 1006–1015. [[CrossRef](#)]
7. Tzampoglou, P.; Loupasakis, C. Evaluating geological and geotechnical data for the study of land subsidence phenomena at the perimeter of the Amyntaio coalmine, Greece. *Int. J. Min. Sci. Technol.* **2017**, *28*, 61–612. [[CrossRef](#)]
8. Mayuga, M. Geology and development of California’s giant-Wilmington oil field. *AAPG Bull.* **1970**, *52*, 540.
9. Papadopoulou-Vrynioti, K.; Bathrellos, G.D.; Skilodimou, H.D.; Kaviris, G.; Makropoulos, K. Karst collapse susceptibility mapping considering peak ground acceleration in a rapidly growing urban area. *Eng. Geol.* **2013**, *158*, 77–88. [[CrossRef](#)]
10. Margiotta, S.; Negri, S.; Parise, M.; Valloni, R. Mapping the susceptibility to sinkholes in coastal areas, based on stratigraphy, geomorphology and geophysics. *Nat. Hazards* **2012**, *62*, 657–676. [[CrossRef](#)]
11. Guerrero, J.; Gutiérrez, F.; Bonachea, J.; Lucha, P. A sinkhole susceptibility zonation based on paleokarst analysis along a stretch of the Madrid–Barcelona high-speed railway built over gypsum-and salt-bearing evaporites (NE Spain). *Eng. Geol.* **2008**, *102*, 62–73. [[CrossRef](#)]
12. Nieuwenhuis, H.; Schokking, F. Land subsidence in drained peat areas of the Province of Friesland, The Netherlands. *Q. J. Eng. Geol. Hydrogeol.* **1997**, *30*, 37–48. [[CrossRef](#)]
13. Choi, J.-K.; Kim, K.-D.; Lee, S.; Won, J.-S. Application of a fuzzy operator to susceptibility estimations of coal mine subsidence in Taebaek City, Korea. *Environ. Earth Sci.* **2010**, *59*, 1009–1022. [[CrossRef](#)]
14. Singh, K.B.; Dhar, B.B. Sinkhole subsidence due to mining. *Geotech. Geol. Eng.* **1997**, *15*, 327–341. [[CrossRef](#)]
15. Gongyu, L.; Wanfang, Z. Sinkholes in karst mining areas in China and some methods of prevention. *Eng. Geol.* **1999**, *52*, 45–50. [[CrossRef](#)]
16. Al Heib, M.; Duval, C.; Theoleyre, F.; Watelet, J.-M.; Gombert, P. Analysis of the historical collapse of an abandoned underground chalk mine in 1961 in Clamart (Paris, France). *Bull. Eng. Geol. Environ.* **2015**, *74*, 1001–1018. [[CrossRef](#)]
17. Terzaghi, K. Settlement and consolidation of clay. In *Principles of Soil Mechanics*; McGraw-Hill: New York, NY, USA, 1925; Volume IV, pp. 874–878.
18. Galloway, D.L.; Burbey, T.J. Review: Regional land subsidence accompanying groundwater extraction. *Hydrogeol. J.* **2011**, *19*, 1459–1486. [[CrossRef](#)]
19. Tsangaratos, P.; Ilija, I.; Loupasakis, C. Land subsidence modelling using data mining techniques. The case study of Western Thessaly, Greece. In *Natural Hazards GIS-Based Spatial Modeling Using Data Mining Techniques*; Pourghasemi, H.P., Rossi, M., Eds.; Springer Nature Switzerland AG: Cham, Switzerland, 2019; pp. 79–103.
20. Hu, R.; Yue, Z.; Wang, L.u.; Wang, S. Review on current status and challenging issues of land subsidence in China. *Eng. Geol.* **2004**, *76*, 65–77. [[CrossRef](#)]
21. Hua, Z.; Tiezhu, L.; Xinhong, L. Economic benefit risk assessment of controlling land subsidence in Shanghai. *Environ. Geol.* **1993**, *21*, 208–211. [[CrossRef](#)]
22. Pramita, A.; Syafrudin, S.; Sugianto, D. Effect of seawater intrusion on groundwater in the Demak coastal area Indonesia: A review. *IOP Conf. Ser. Earth Environ. Sci.* **2021**, *896*, 012070. [[CrossRef](#)]
23. Abidin, H.; Andreas, H.; Gumilar, I.; Sidiq, T.P.; Fukuda, Y. Land subsidence in coastal city of Semarang (Indonesia): Characteristics, impacts and causes. *Geomat. Nat. Hazards Risk* **2013**, *4*, 226–240. [[CrossRef](#)]
24. Purwoarminta, A.; Moosdorf, N.; Delinom, R.M. Investigation of groundwater-seawater interactions: A review. *IOP Conf. Ser. Earth Environ. Sci.* **2018**, *118*, 012017. [[CrossRef](#)]
25. Ireland, R.; Poland, J.; Riley, F. Land Subsidence in the San Joaquin Valley, California, as of 1980. *US Geol. Surv. Prof. Pap.* **1984**, *437*, 93.
26. Abidin, H.Z.; Djaja, R.; Darmawan, D.; Hadi, S.; Akbar, A.; Rajiyowiryono, H.; Sudiby, Y.; Meilano, I.; Kasuma, M.; Kahar, J. Land subsidence of Jakarta (Indonesia) and its geodetic monitoring system. *Nat. Hazards* **2001**, *23*, 365–387. [[CrossRef](#)]
27. Cenni, N.; Fiaschi, S.; Fabris, M. Monitoring of land subsidence in the po river delta (Northern Italy) using geodetic networks. *Remote Sens.* **2021**, *13*, 1488. [[CrossRef](#)]
28. Tiwari, A.; Narayan, A.B.; Dwivedi, R.; Swadeshi, A.; Pasari, S.; Dikshit, O. Geodetic investigation of landslides and land subsidence: Case study of the Bhurkunda coal mines and the Sirobagarh landslide. *Surv. Rev.* **2020**, *52*, 134–149. [[CrossRef](#)]
29. Colesanti, C.; Ferretti, A.; Prati, C.; Rocca, F. Monitoring landslides and tectonic motions with the Permanent Scatterers Technique. *Eng. Geol.* **2003**, *68*, 3–14. [[CrossRef](#)]
30. Donnelly, L. Fault reactivation induced by mining in the East Midlands. *Mercian Geol.* **2000**, *15*, 29–36.
31. Burbey, T.J. The influence of faults in basin-fill deposits on land subsidence, Las Vegas Valley, Nevada, USA. *Hydrogeol. J.* **2002**, *10*, 525–538. [[CrossRef](#)]
32. Xue, Y.-Q.; Zhang, Y.; Ye, S.-J.; Wu, J.-C.; Li, Q.-F. Land subsidence in China. *Environ. Geol.* **2005**, *48*, 713–720. [[CrossRef](#)]
33. Kim, K.-D.; Lee, S.; Oh, H.-J.; Choi, J.-K.; Won, J.-S. Assessment of ground subsidence hazard near an abandoned underground coal mine using GIS. *Environ. Geol.* **2006**, *50*, 1183–1191. [[CrossRef](#)]
34. Motagh, M.; Walter, T.R.; Sharifi, M.A.; Fielding, E.; Schenk, A.; Anderssohn, J.; Zschau, J. Land subsidence in Iran caused by widespread water reservoir overexploitation. *Geophys. Res. Lett.* **2008**, *35*, L16403. [[CrossRef](#)]

35. Huang, B.; Shu, L.; Yang, Y. Groundwater overexploitation causing land subsidence: Hazard risk assessment using field observation and spatial modelling. *Water Resour. Manag.* **2012**, *26*, 4225–4239. [CrossRef]
36. Yan, Y.; Doin, M.-P.; Lopez-Quiroz, P.; Tupin, F.; Fruneau, B.; Pinel, V.; Trouvé, E. Mexico city subsidence measured by InSAR time series: Joint analysis using PS and SBAS approaches. *IEEE J. Sel. Top. Appl. Earth Obs. Remote Sens.* **2012**, *5*, 1312–1326. [CrossRef]
37. Pacheco-Martínez, J.; Hernández-Marín, M.; Burbey, T.J.; González-Cervantes, N.; Ortiz-Lozano, J.Á.; Zermeño-De-Leon, M.E.; Solís-Pinto, A. Land subsidence and ground failure associated to groundwater exploitation in the Aguascalientes Valley, Mexico. *Eng. Geol.* **2013**, *164*, 172–186. [CrossRef]
38. Loupasakis, C.; Angelitsa, V.; Rozos, D.; Spanou, N. Mining geohazards—Land subsidence caused by the dewatering of opencast coal mines: The case study of the Amyntaio coal mine, Florina, Greece. *Nat. Hazards* **2014**, *70*, 675–691. [CrossRef]
39. Tzampoglou, P.; Loupasakis, C. Numerical simulation of the factors causing land subsidence due to overexploitation of the aquifer in the Amyntaio open coal mine, Greece. *HydroResearch* **2019**, *1*, 8–24. [CrossRef]
40. Council on Environmental Quality. *Contamination of Ground Water by Toxic Organic Chemicals*; Council on Environmental Quality: Washington, DC, USA, 1981.
41. Leeden, F.d.; Troise, F.L.; Todd, D.K. *The Water Encyclopedia*; Lewin Publishers: Boca Raton, FL, USA, 1990.
42. Mindling, A. *A Summary of Data Relating to Land Subsidence in Las Vegas Valley*; Center for Water Resources Research, University of Nevada System: Reno, NV, USA, 1971.
43. Wood, D.B. Water use and associated effects on ground-water levels, Las Vegas Valley and vicinity, Clark County, Nevada, 1980–1995. *Nev. Div. Water Resour. Inf.* **1999**, *35*, 101.
44. Maxey, G.; Jameson, C. Geology and Water resources of Las Vegas, Pahump and Indian Springs Valleys, Clark and Nye County, Nevada, State of Nevada: Office of the State Engineer. *Water Resour. Bull.* **1948**, 292. Available online: https://data.nbmng.unr.edu/public/Geothermal/GreyLiterature/Maxey_SouthernNVResources_1948.pdf (accessed on 9 December 2021).
45. Amelung, F.; Galloway, D.L.; Bell, J.W.; Zebker, H.A.; Lacznia, R.J. Sensing the ups and downs of Las Vegas: InSAR reveals structural control of land subsidence and aquifer-system deformation. *Geology* **1999**, *27*, 483–486. [CrossRef]
46. Bell, J.W.; Amelung, F.; Ramelli, A.R.; Blewitt, G. Land subsidence in Las Vegas, Nevada, 1935–2000: New geodetic data show evolution, revised spatial patterns, and reduced rates. *Environ. Eng. Geosci.* **2002**, *8*, 155–174. [CrossRef]
47. Zhang, B.; Zhang, L.; Yang, H.; Zhang, Z.; Tao, J. Subsidence prediction and susceptibility zonation for collapse above goaf with thick alluvial cover: A case study of the Yongcheng coalfield, Henan Province, China. *Bull. Eng. Geol. Environ.* **2016**, *75*, 1117–1132. [CrossRef]
48. Bell, J.W. Las Vegas Valley: Land Subsidence and Fissuring Due to Ground-Water Withdrawal. Available online: https://geochange.er.usgs.gov/sw/impacts/hydrology/vegas_gw/ (accessed on 9 December 2021).
49. Thompson, E. *Alternatives for Future Urban Growth in California's Central Valley: The Bottom Line for Agriculture and Taxpayers*; AFT's California Field Office: Davis, CA, USA, 1995; p. 139.
50. Poland, J.; Davis, G. Subsidence of the land surface in the Tulare-Wasco (Delano) and Los Banos-Kettleman City area, San Joaquin Valley, California. *Eos Trans. Am. Geophys. Union* **1956**, *37*, 287–296. [CrossRef]
51. Ireland, R.; Poland, J.; Riley, F.S. *Land Subsidence in the San Joaquin Valley, California, as of 1980*; U.S. Geological Survey Professional Paper 437-I; U.S. Department of the Interior: Washington, DC, USA, 1984. [CrossRef]
52. Poland, J.F. The Occurrence and Control of Land Subsidence due to Ground-Water Withdrawal with Special Reference to the San Joaquin and Santa Clara Valleys, California. Ph.D. Thesis, Department of Geology, Stanford University, Stanford, CA, USA, 1981.
53. Larson, K.; Başağaoğlu, H.; Marino, M. Prediction of optimal safe ground water yield and land subsidence in the Los Banos-Kettleman City area, California, using a calibrated numerical simulation model. *J. Hydrol.* **2001**, *242*, 79–102. [CrossRef]
54. Jeanne, P.; Farr, T.G.; Rutqvist, J.; Vasco, D.W. Role of agricultural activity on land subsidence in the San Joaquin Valley, California. *J. Hydrol.* **2019**, *569*, 462–469. [CrossRef]
55. Ojha, C.; Werth, S.; Shirzaei, M. Groundwater loss and aquifer system compaction in San Joaquin Valley during 2012–2015 drought. *J. Geophys. Res. Solid Earth* **2019**, *124*, 3127–3143. [CrossRef]
56. Location of Maximum Land Subsidence in, U.S. Levels at 1925 and 1977. Available online: <https://www.usgs.gov/media/images/location-maximum-land-subsidence-us-levels-1925-and-1977> (accessed on 9 December 2021).
57. Energy Resources. Available online: www.longbeach.gov/lbgo/about-us/oil/subsidence/ (accessed on 9 December 2021).
58. Tolman, C.F.; Poland, J.F. *Land Subsidence in the San Joaquin Valley, California, as of 1972*; U.S. Geological Survey Professional Paper; U.S. Department of the Interior: Washington, DC, USA, 1975; p. 78. [CrossRef]
59. Galloway, D.L.; Jones, D.R.; Ingebritsen, S.E. *Land subsidence in the United States*; US Geological Survey: Reston, VA, USA, 1999; Volume 1182.
60. Holzer, T.L.; Galloway, D.L. Impacts of land subsidence caused by withdrawal of underground fluids in the United States. *Rev. Eng. Geol.* **2005**, *16*, 87–99.
61. Fowler, L.C. Economic consequences of land subsidence. *Am. Soc. Civ. Eng. J. Irrig.* **1981**, *107*, 151–159.
62. McComb, D. *Houston, Texas, in The New Handbook of Texas*; Tyler, R., Barnett, D.E., Barkley, R.R., Eds.; Texas State Historical Association: Austin, TX, USA, 1996; pp. 1–3.
63. Buckley, S.M.; Rosen, P.A.; Hensley, S.; Tapley, B.D. Land subsidence in Houston, Texas, measured by radar interferometry and constrained by extensometers. *J. Geophys. Res. Solid Earth* **2003**, *108*, 2542. [CrossRef]
64. Coplin, L.S.; Galloway, D. Houston-Galveston, Texas. Land subsidence in the United States. *US Geol. Surv. Circ.* **1999**, *1182*, 35–48.

65. Galloway, D.L.; Coplin, L.S.; Ingebritsen, S.E. Effects of land subsidence in the Greater Houston area. *Manag. Urban Water Supply* **2003**, *46*, 187–203.
66. Shah, S.D.; Ramage, J.K.; Braun, C.L. *Status of Groundwater-Level Altitudes and Long-Term Groundwater-Level Changes in the Chicot, Evangeline, and Jasper Aquifers, Houston-Galveston Region, Texas, 2018*; 2328-0328; US Geological Survey: Liston, VA, USA, 2018.
67. Agudelo, G.; Wang, G.; Liu, Y.; Bao, Y.; Turco, M.J. GPS geodetic infrastructure for subsidence and fault monitoring in Houston, Texas, USA. *Proc. Int. Assoc. Hydrol. Sci.* **2020**, *382*, 11–18. [[CrossRef](#)]
68. Miller, M.M.; Shirzaei, M. Land subsidence in Houston correlated with flooding from Hurricane Harvey. *Remote Sens. Environ.* **2019**, *225*, 368–378. [[CrossRef](#)]
69. Radar Interferometry Measurement of Land Subsidence in Houston, Texas (Photographer: S. Duncan Heron). Available online: https://www.csr.utexas.edu/rs/research/insar/houston_desc.html (accessed on 9 December 2021).
70. Carpenter, M.C. South-Central Arizona: Earth fissures and subsidence complicate development of desert water resources. *Land Subsidence. United States US Geol. Surv. Circ.* **1999**, *1182*, 65–78.
71. ADWR. *Groundwater Sites Inventory (GWSI)*; Arizona Department of Water Resources: Phoenix, AZ, USA, 2015.
72. ADWR. *Land Subsidence Maps*; Arizona Department of Water Resources: Phoenix, AZ, USA, 2015.
73. Schumann, H.H.; O'Day, C.M. *Investigation of Hydrogeology, Land Subsidence, and Earth Fissures, Luke Air Force Base, Arizona*; Administrative Report; US Geological Survey: Tucson, AZ, USA, 1995.
74. Schumann, H.H.; Genualdi, R.B. *Land Subsidence, Earth Fissures, and Water-Level Change in Southern Arizona*; Arizona Bureau of Geology and Mineral Technology: Tucson, AZ, USA, 1986.
75. Conway, B. *Arizona Department of Water Resources Land Subsidence Monitoring Report Number 2*; ADWR: Phoenix, AZ, USA, 2014.
76. Conway, B.D. Arizona Department of Water Resources Land Subsidence Monitoring Program. In Proceedings of the IAEG/AEG Annual Meeting Proceedings, San Francisco, CA, USA, 17–21 September 2018; Springer Nature: Cham, Switzerland, 2019; Volume 5, pp. 61–67.
77. Conway, B.D. Land subsidence and earth fissures in south-central and southern Arizona, USA. *Hydrogeol. J.* **2016**, *24*, 649–655. [[CrossRef](#)]
78. AZGS. Locations of mapped earth fissure traces in Arizona, v. 01.29.2015. In *Arizona Geological Survey Digital Information*; AZGS: Tucson, AZ, USA, 2015.
79. Subsidence Cracks & Fissures, Cochise Co., Arizona—October 2011 (Photographer: Jan Rasmussen). Available online: <https://arizonageologicalsoc.org/SubsidenceFissures/> (accessed on 9 December 2021).
80. Cracks in Arizona. Available online: http://azgeology.azgs.arizona.edu/archived_issues/azgs.az.gov/arizona_geology/april09/article_cracksinaz.html (accessed on 9 December 2021).
81. Keller, E.; Blodgett, R. *Natural Hazards: Earth's Processes as Hazards, Disasters, and Catastrophes*; Pentice Hall: Hoboken, NJ, USA, 2006.
82. Instituto Nacional de Estadística Geografía e Informática. *Censo Nacional de Población, 2010, Mexico*; Instituto Nacional de Estadística, Geografía e Informática: Mexico City, Mexico, 2011.
83. Leake, S. Interbed storage changes and compaction in models of regional groundwater flow. *Water Resour. Res.* **1990**, *26*, 1939–1950. [[CrossRef](#)]
84. Chaussard, E.; Wdowinski, S.; Cabral-Cano, E.; Amelung, F. Land subsidence in central Mexico detected by ALOS InSAR time-series. *Remote Sens. Environ.* **2014**, *140*, 94–106. [[CrossRef](#)]
85. Marsal, R.; Hiriart, F.; Sandoval, L. Hundimiento de la ciudad de México. Observaciones y estudios analíticos. *ICA Ser. B Ing. Exp.* **1952**, *3*, 1–26.
86. Custodio, E. Aquifer overexploitation: What does it mean? *Hydrogeol. J.* **2002**, *10*, 254–277. [[CrossRef](#)]
87. Aguilar-Pérez, L.A.; Ortega-Guerrero, M.A.; Lugo-Hubp, J.; Ortiz-Zamora, D.d.C. Análisis numérico acoplado de los desplazamientos verticales y generación de fracturas por extracción de agua subterránea en las proximidades de la Ciudad de México. *Rev. Mex. de Cienc. Geológicas* **2006**, *23*, 247–261.
88. Cabral-Cano, E.; Dixon, T.H.; Miralles-Wilhelm, F.; Díaz-Molina, O.; Sánchez-Zamora, O.; Carande, R.E. Space geodetic imaging of rapid ground subsidence in Mexico City. *Geol. Soc. Am. Bull.* **2008**, *120*, 1556–1566. [[CrossRef](#)]
89. Cuevas, J.A. Foundation conditions in Mexico City. In Proceedings of the International Conference on Soil Mechanics; Graduate school of engineering, Harvard University: Cambridge, MA, USA, 1936; pp. 233–237.
90. Juárez, B. Mecanismo de Las Grietas de Tensión en el Valle de México. Ph.D. Thesis, Universidad Nacional Autónoma de México, Mexico City, Mexico. Available online: <https://repositorio.unam.mx/contenidos/888291961> (accessed on 9 December 2021).
91. Marsal, R. Development of a lake by pumping-induced consolidation of soft clays. *Vol. Nabor Carrillo Com. Impuls. Y Coord. De La Investig. Cient.* **1969**, *47*, 229–266.
92. Marsal, R.; Mazari, M. *The Subsoil of Mexico City: México*; Escuela de Ingeniería, Vol. I y II; Universidad Nacional Autónoma de México: Mexico City, Mexico, 1959.
93. Ortiz-Zamora, D.; Ortega-Guerrero, A. Evolution of long-term land subsidence near Mexico City: Review, field investigations, and predictive simulations. *Water Resour. Res.* **2010**, *46*, 1. [[CrossRef](#)]
94. Haner, J. Sinking of Mexico City linked to Metro Accident, with More to Come. Available online: <https://www.science.org/content/article/sinking-mexico-city-linked-metro-accident-more-come> (accessed on 9 December 2021).

95. Land Subsidence in Mexico City Observed by InSAR. Available online: https://topex.ucsd.edu/rs/term_YaoYu.pdf (accessed on 9 December 2021).
96. Mazari, M.; Alberro, J. Hundimiento de la Ciudad de México. In *Problemas de la Cuenca de México*; El Colegio Nacional: Ciudad de México, Mexico, 1990; pp. 83–114.
97. Ortega-Guerrero, A.; Rudolph, D.L.; Cherry, J.A. Analysis of long-term land subsidence near Mexico City: Field investigations and predictive modeling. *Water Resour. Res.* **1999**, *35*, 3327–3341. [[CrossRef](#)]
98. Vega, F.G.E. Subsidence of the city of Mexico: A historical review. In Proceedings of the Second International Symposium on land Subsidence, Anaheim, CA, USA, 13–17 December 1976; International Association of Hydrological Science: Wallingford, UK, 1976; pp. 35–38.
99. Cabral-Cano, E.; Arciniega-Ceballos, A.; Díaz-Molina, O.; Cigna, F.; Osmanoglu, B.; Dixon, T.; DeMets, C.; Vergara-Huerta, F.; Garduño-Monroy, V.; Ávila-Olivera, J. Is there a tectonic component on the subsidence process in Morelia, Mexico. In Proceedings of the Land Subsidence, Associated Hazards and the Role of Natural Resources Development, Querétaro, Mexico, 17–22 October 2010; IAHS Press: Wallingford, UK, 2010; pp. 164–169.
100. Cabral-Cano, E.; Osmanoglu, B.; Dixon, T.; Wdowinski, S.; DeMets, C.; Cigna, F.; Díaz-Molina, O. Subsidence and fault hazard maps using PSI and permanent GPS networks in central Mexico. In Proceedings of the Eighth International Symposium on Land Subsidence, Querétaro, Mexico, 17–22 October 2010; pp. 17–22.
101. López-Quiroz, P.; Doin, M.-P.; Tupin, F.; Briole, P.; Nicolas, J.-M. Time series analysis of Mexico City subsidence constrained by radar interferometry. *J. Appl. Geophys.* **2009**, *69*, 1–15. [[CrossRef](#)]
102. Osmanoglu, B.; Dixon, T.H.; Wdowinski, S.; Cabral-Cano, E.; Jiang, Y. Mexico City subsidence observed with persistent scatterer InSAR. *Int. J. Appl. Earth Obs. Geoinf.* **2011**, *13*, 1–12. [[CrossRef](#)]
103. Strozzi, T.; Wegmuller, U.; Werner, C.L.; Wiesmann, A.; Spreckels, V. JERS SAR interferometry for land subsidence monitoring. *IEEE Trans. Geosci. Remote Sens.* **2003**, *41*, 1702–1708. [[CrossRef](#)]
104. Strozzi, T.; Werner, C.; Wegmuller, U.; Wiesmann, A. Monitoring land subsidence in Mexico City with Envisat ASAR Interferometry. In Proceedings of the Envisat & ERS Symposium, Salzburg, Austria, 6–10 September 2004; p. 154.
105. Strozzi, T.; Wegmuller, U. Land subsidence in Mexico City mapped by ERS differential SAR interferometry. In Proceedings of the Geoscience and Remote Sensing Symposium—IGARSS'99 (Cat. No.99CH36293), Hamburg, Germany, 28 June–2 July 1999; pp. 1940–1942. [[CrossRef](#)]
106. Solano-Rojas, D.E.; Wdowinski, S.; Cabral-Cano, E.; Osmanoglu, B.; Havazli, E.; Pacheco-Martínez, J. A multiscale approach for detection and mapping differential subsidence using multi-platform InSAR products. *Proc. Int. Assoc. Hydrol. Sci.* **2020**, *382*, 173–177. [[CrossRef](#)]
107. Fernández-Torres, E.; Cabral-Cano, E.; Solano-Rojas, D.; Havazli, E.; Salazar-Tlaczani, L. Land Subsidence risk maps and InSAR based angular distortion structural vulnerability assessment: An example in Mexico City. *Proc. Int. Assoc. Hydrol. Sci.* **2020**, *382*, 583–587. [[CrossRef](#)]
108. Poreh, D.; Pirasteh, S.; Cabral-Cano, E. Assessing subsidence of Mexico City from InSAR and LandSat ETM+ with CGPS and SVM. *Geoenviron. Disasters* **2021**, *8*, 1–19. [[CrossRef](#)]
109. Cigna, F.; Tapete, D. Sentinel-1 InSAR Survey to Constrain Subsidence-Induced Surface Faulting and Quantify its Induced Risk in Major Cities of Central Mexico, EGU General Assembly 2021, online, 19–30 April 2021; EGU21-15723. Available online: <https://meetingorganizer.copernicus.org/EGU21/EGU21-15723.html?pdf> (accessed on 9 December 2021).
110. Rodríguez-Castillo, R. Social-environmental impact of the extraction policy of the Guaymas Valley aquifer, Sonora, Mexico. *Aquifer Overexploit. Int. Assoc. Hydrogeol. Sel. Pap.* **1993**, *3*, 293–302.
111. Comisión Nacional del Agua. *Cuantificación de la extracción del Agua Subterránea en el Valle de Celaya, Gto., Aplicando Técnicas de Percepción Remota. Contrato 2458*; Gonwana Exploraciones. S.A., C.V., Comisión Nacional del Agua: Mazatlán, Mexico, 2004; p. 100.
112. Huizar-Álvarez, R.; Mitre-Salazar, L.M.; Marín-Córdova, S.; Trujillo-Candelaria, J.; Martínez-Reyes, J. Subsidence in Celaya, Guanajuato, Central Mexico: Implications for groundwater extraction and the neotectonic regime. *Geofísica Int.* **2011**, *50*, 255–270. [[CrossRef](#)]
113. Avila-Olivera, J.A.; Farina, P.; Garduño-Monroy, V.H. Integration of InSAR and GIS in the Study of Surface Faults Caused by Subsidence-Creep-Fault Processes in Celaya, Guanajuato, Mexico. *AIP Conf. Proc.* **2008**, *1009*, 200–211. [[CrossRef](#)]
114. Farina, P.; Avila-Olivera, J.A.; Garduño-Monroy, V.H. Structurally-controlled urban subsidence along the Mexican Volcanic Belt (MVB) monitored by InSAR. In Proceedings of the Envisat Symposium 2007, Montreux, Switzerland, 23–27 April 2007.
115. Farina, P.; Avila-Olivera, J.A.; Garduño-Monroy, V.H.; Catani, F. DInSAR analysis of differential ground subsidence affecting urban areas along the Mexican Volcanic Belt (MVB). *Riv. Ital. Telerilevamento (AIT) Il Telerilevamento Microonde L'attività Ric. Appl.* **2008**, *40*, 103–113. [[CrossRef](#)]
116. Castellazzi, P.; Arroyo-Domínguez, N.; Martel, R.; Calderhead, A.I.; Normand, J.C.; Gárfias, J.; Rivera, A. Land subsidence in major cities of Central Mexico: Interpreting InSAR-derived land subsidence mapping with hydrogeological data. *Int. J. Appl. Earth Obs. Geoinf.* **2016**, *47*, 102–111. [[CrossRef](#)]
117. Aguirre, G.; Zúñiga, R.; Pacheco, J.; Guzmán, M.; Nieto, J. El graben de Querétaro México. *Obs. Fallamiento Act. GEOS* **2000**, *20*, 2–7.

118. Garduno, V.H.; Arreygue, R.E.; Israde, I.; Rodriguez, G.M. Efecto de las fallas asociadas a la sobreexplotación de acuíferos y la presencia de fallas potencialmente sísmicas en Morelia, Michoacan, Mexico. *Rev. Mex. Cienc. Geol.* **2001**, *18*, 37–54.
119. Cigna, F.; Cabral-Cano, E.; Osmanoglu, B.; Dixon, T.H.; Wdowinski, S. Detecting subsidence-induced faulting in Mexican urban areas by means of Persistent Scatterer Interferometry and subsidence horizontal gradient mapping. In Proceedings of the Geoscience and Remote Sensing Symposium (IGARSS), Vancouver, Canada, 24–29 July 2011; pp. 2125–2128.
120. Cigna, F.; Osmanoglu, B.; Cabral-Cano, E.; Dixon, T.H.; Ávila-Olivera, J.A.; Garduño-Monroy, V.H.; DeMets, C.; Wdowinski, S. Monitoring land subsidence and its induced geological hazard with Synthetic Aperture Radar Interferometry: A case study in Morelia, Mexico. *Remote Sens. Environ.* **2012**, *117*, 146–161. [[CrossRef](#)]
121. Figueroa-Miranda, S.; Hernández-Madrigal, V.M.; Tuxpan-Vargas, J.; Villaseñor-Reyes, C.I. Evolution assessment of structurally-controlled differential subsidence using SBAS and PS interferometry in an emblematic case in Central Mexico. *Eng. Geol.* **2020**, *279*, 105860. [[CrossRef](#)]
122. Cigna, F.; Tapete, D. Urban growth and land subsidence: Multi-decadal investigation using human settlement data and satellite InSAR in Morelia, Mexico. *Sci. Total Environ.* **2022**, *811*, 152211. [[CrossRef](#)] [[PubMed](#)]
123. López-Doncel, R.; Mata-Segura, J.; Cruz-Márquez, J.; Arzate-Flores, J.; Pacheco-Martínez, J. Geological risk to the historical heritage. Examples of the historic center of the city of San Luis Potosí (Riesgo geológico para el patrimonio histórico. Ejemplos del centro histórico de la ciudad de San Luis Potosí). *Boletín Soc. Geológica Mex.* **2006**, *58*, 259–263. [[CrossRef](#)]
124. Lin, Z.D. Analysis of development of groundwater in China. *Hydrology* **2004**, *24*, 18–21.
125. Huang, F.; Wang, G.; Yang, Y.; Wang, C. Overexploitation status of groundwater and induced geological hazards in China. *Nat. Hazards* **2014**, *73*, 727–741. [[CrossRef](#)]
126. He, Q.; Ye, X.; Liu, W.; Li, Z.; Li, C. Land subsidence in the northern china plain (NCP). In Proceedings of the 7th Int Symp Land Subsidence (SISLOS 2005), Shanghai, China, 23–28 October 2005; pp. 18–29.
127. Ye, S.; Xue, Y.; Wu, J.; Yan, X.; Yu, J. Progression and mitigation of land subsidence in China. *Hydrogeol. J.* **2016**, *24*, 685–693. [[CrossRef](#)]
128. Chai, J.; Shen, S.; Zhu, H.; Zhang, X. Land subsidence due to groundwater drawdown in Shanghai. *Geotechnique* **2004**, *54*, 143–147. [[CrossRef](#)]
129. Han, J.M. Land subsidence and its counter measures of control in Shandong Province. *Chin. J. Geol. Hazard Control* **1998**, *9*, 33–35. (In Chinese)
130. Shen, S.; Tohno, I.; Nishgaki, M.; Miura, N. Land subsidence due to withdrawal of deep-groundwater. *Lowl. Technol. Int.* **2004**, *6*, 1–8.
131. Wu, T.J.; Cui, X.D.; Niu, X.J.; Chen, W.J. A study and prevention about land subsidence in Tianjin City. *Hydrogeol. Eng. Geol.* **1998**, *5*, 17–20.
132. Zhang, A.G.; Wei, Z.X. Prevention and cure with Shanghai land subsidence and city sustaining development. In Proceedings of the 7th Int Symp Land Subsidence (SISLOS 2005), Shanghai, China, 23–28 October 2005; pp. 10–17.
133. Gong, S. Change of groundwater seepage field and its influence on development of land subsidence in Shanghai. *J. Water Resour. Water Eng.* **2009**, *20*, 1–6.
134. Li, Q.; Wang, H. A study on land subsidence in Shanghai. *Geol. J. China Univ.* **2006**, *12*, 169–178.
135. Niu, X.; Ying, Y.; Bai, J.; Ma, F. Secondary-consolidation deformation of soil and its effects on subsidence in Tianjin. In Proceedings of the 7th Int Symp Land Subsidence (SISLOS 2005), Shanghai, China, 23–28 October 2005; pp. 88–96.
136. Wang, H.G. Current Situation and Tendency of Land Subsidence in Tianjin. Master's Thesis, China University of Geosciences, Wuhan, China, 2006; pp. 26–32.
137. Wei, J.S.; Xu, J.; Lu, Y.; Yi, C.R. Analysis on land subsidence funnel in Wangqingtu area of Tianjin. *Ground Water* **2012**, *34*, 49–51.
138. Ma, T.; Wang, Y.; Yan, S.; Ma, R.; Yan, C.; Zhou, X. Causes of land subsidence in Taiyuan city, Shanxi, China. In Proceedings of the 7th Int Symp Land Subsidence (SISLOS 2005), Shanghai, China, 23–28 October 2005; pp. 102–110.
139. Yu-hai, L.; Zhi-xin, C.; Wan-kui, N. A study on hazard-Forming mechanisms of geofracture and land subsidence and control countermeasure in Xi'an. *Chin. J. Geol. Hazard Control* **1994**, *5*, 67–74.
140. Zhang, X. On establishment of Suzhou earth subsidence gray forecast model. *J. Suzhou Inst. Urban Constr. Environ. Prot.* **2000**, *13*, 53–57.
141. Zhang, Z.Y. Analysis on present situation and development trend of groundwater descent funnel in Cangzhou City. *Ground Water* **2007**, *29*, 50–53.
142. Yiping, W. Study on land subsidence caused by overexploiting groundwater in Beijing. *Site Investig. Sci. Technol.* **2004**, *5*, 46–49.
143. Miao, X.; Zhu, X.; Lu, M.; Chen, F.; Huangpu, A. Study of water exploitation and land subsidence control in Su–Xi–Chang area. *Chin. J. Geol. Hazard Control* **2007**, *18*, 132–139.
144. He, X.-C.; Yang, T.-L.; Shen, S.-L.; Xu, Y.-S.; Arulrajah, A. Land subsidence control zone and policy for the environmental protection of Shanghai. *Int. J. Environ. Res. Public Health* **2019**, *16*, 2729. [[CrossRef](#)]
145. Li, J.; Zhou, L.; Ren, C.; Liu, L.; Zhang, D.; Ma, J.; Shi, Y. Spatiotemporal Inversion and Mechanism Analysis of Surface Subsidence in Shanghai Area Based on Time-Series InSAR. *Appl. Sci.* **2021**, *11*, 7460. [[CrossRef](#)]
146. Li, C.; Tang, X.; Ma, T. Land subsidence caused by groundwater exploitation in the Hangzhou-Jiaxing-Huzhou Plain, China. *Hydrogeol. J.* **2006**, *14*, 1652–1665. [[CrossRef](#)]

147. Jiang, Y.; Tian, F.; Luo, Y.; Wang, F.; Yang, Y. Research on the relationship between groundwater level and layered subsidence in typical regions of Beijing. *South N Water Transf. Water Sci. Technol.* **2015**, *13*, 95–99.
148. Yang, Y.; Jia, S.; Wang, H. The status and development of land subsidence in Beijing Plain. *Shanghai Geol.* **2010**, *31*, 23–28.
149. Dong, J.; Guo, S.; Wang, N.; Zhang, L.; Ge, D.; Liao, M.; Gong, J. Tri-decadal evolution of land subsidence in the Beijing Plain revealed by multi-epoch satellite InSAR observations. *Remote Sens. Environ.* **2023**, *286*, 113446. [[CrossRef](#)]
150. Li, S.F.; Ye, X.B.; He, Q.C.; Fang, H.; She, W.F. A discussion on evaluation method of economical losing due to land subsidence hazard in North China Plain. *Hydrogeol. Eng. Geol.* **2006**, *4*, 114–116.
151. Hu, L.; Dai, K.; Xing, C.; Li, Z.; Tomás, R.; Clark, B.; Shi, X.; Chen, M.; Zhang, R.; Qiu, Q. Land subsidence in Beijing and its relationship with geological faults revealed by Sentinel-1 InSAR observations. *Int. J. Appl. Earth Obs. Geoinf.* **2019**, *82*, 101886. [[CrossRef](#)]
152. Chen, B.; Gong, H.; Chen, Y.; Li, X.; Zhou, C.; Lei, K.; Zhu, L.; Duan, L.; Zhao, X. Land subsidence and its relation with groundwater aquifers in Beijing Plain of China. *Sci. Total Environ.* **2020**, *735*, 139111. [[CrossRef](#)] [[PubMed](#)]
153. Li, M.L. Mechanism and solutions of land subsidence on the plain areas of the southern part of Beijing-Tianjin on North China Plain. *J. Water Sci. Technol. Water Transf. Proj. South-North Water* **2006**, *4*, 52–53.
154. Li, D.; Hou, X.; Song, Y.; Zhang, Y.; Wang, C. Ground subsidence analysis in Tianjin (China) based on Sentinel-1A data using MT-InSAR methods. *Appl. Sci.* **2020**, *10*, 5514. [[CrossRef](#)]
155. Zhao, R.; Wang, G.; Yu, X.; Sun, X.; Bao, Y.; Xiao, G.; Gan, W.; Shen, S. Rapid land subsidence in Tianjin, China derived from continuous GPS observations (2010–2019). *Proc. Int. Assoc. Hydrol. Sci.* **2020**, *382*, 241–247. [[CrossRef](#)]
156. Lixin, Y.; Jie, W.; Chuanqing, S.; Guo, J.-W.; Yanxiang, J.; Liu, B. Land subsidence disaster survey and its economic loss assessment in Tianjin, China. *Nat. Hazards Rev.* **2010**, *11*, 35–41. [[CrossRef](#)]
157. Zhang, Y.X. Primary research on forecasting problem of time sequence in geotechnical engineering. *Chin. J. Rock Mech. Eng.* **1998**, *17*, 552–558.
158. Lv, F.; Ma, X.; Zhao, C.; Song, W. The distribution and causes of ground fissures on the Hebei Plain. *Shanghai Land Resour.* **2014**, *35*, 49–53.
159. Suo, C.; Wang, D.; Liu, Z. Land fissures and subsidence prevention in Xi'an. *Quat. Sci.* **2005**, *25*, 23–28.
160. Lee, C.F.; Zhang, J.M.; Zhang, Y.X. Evolution and origin of the ground fissures in Xian, China. *Eng. Geol.* **1996**, *43*, 45–55. [[CrossRef](#)]
161. Ohgaki, S.; Takizawa, S.; Kataoka, Y.; Kuyama, T.; Herath, G.; Hara, K.; Kathiwada, N.R.; Moon, H.J. *Sustainable Groundwater Management in Asian Cities: A final report of Research on Sustainable Water Management Policy*; Institute for Global Environmental Strategies: Hayama, Japan, 2007; p. 157.
162. UNEP; BGS; DGDC; DFID. *Groundwater and its Susceptibility to Degradation: A Global Assessment of the Problem and Options for Management*, UNEP/DEWA/RS.03-3; United Nation Environment Program: Nairobi, Kenya, 2003; p. 126.
163. Ishii, M.; Kuramochi, F.; Endo, T. Recent tendencies of the land subsidence in Tokyo. In Proceedings of the Anaheim Symposium, Anaheim, CA, USA, 12–13 February 1976; Association for Computing Machinery: New York, NY, USA, 1976; pp. 25–34.
164. Onodera, S.; Saito, M. Approaches to estimation of contaminant load variation at Mega-cities. In Proceedings of the RIHN International Symposium on Human Impacts on Urban Subsurface Environments, Kyoto, Japan, 18–20 October 2005; p. 325.
165. Shindo, S. Urban groundwater. Hydrol. In *Hydrological Environment in Urban Area*; Kyoritsu Shuppan: Tokyo, Japan, 1987; pp. 109–154.
166. Yamamoto, S. Recent trend of land subsidence in Japan. In Proceedings of the second International Symposium on Land subsidence, Anaheim, CA, USA, 13–17 December 1976; pp. 9–15.
167. Sato, C.; Haga, M.; Nishino, J. Land subsidence and groundwater management in Tokyo. *Int. Rev. Environ. Strateg.* **2006**, *6*, 403–424.
168. Hayashi, T.; Tokunaga, T.; Taichi, M.; Shimada, J.; Taniguchi, M. Effects of human activities and urbanization on groundwater environments: An example from the aquifer system of Tokyo and the surrounding area. *Sci. Total Environ.* **2009**, *407*, 3165–3172. [[CrossRef](#)] [[PubMed](#)]
169. Gallardo, A.H.; Marui, A.; Takeda, S.; Okuda, F. Groundwater supply under land subsidence constrains in the Nobi Plain. *Geosci. J.* **2009**, *13*, 151–159. [[CrossRef](#)]
170. Iida, K.; Sazanami, T.; Kuwahara, T.; Ueshita, K. *Subsidence of the Nobi Plain*; International Association Hydrogeological Sciences: Wallingford, UK, 1977; pp. 47–54.
171. Yamamoto, S. Case History No. 9.6. Nobi Plain, Japan. In *Guidebook to Studies of Land Subsidence due to Ground-Water Withdrawal*; Poland, J.F., Ed.; United Nations Educational, Scientific and Cultural Organization: Ann Arbor, MI, USA, 1984; pp. 194–204.
172. Ministry of Economy; Trade and Industry of Japan. Survey on the rational use of groundwater in the city of Kaizu, Gifu prefecture. In *Report to the Bureau of the Ministry of Economy in Central Japan*; Bureau of the Ministry of Economy in Central Japan: Tokyo, Japan, 2006; p. 117.
173. Abidin, H.Z.; Andreas, H.; Djaja, R.; Darmawan, D.; Gamal, M. Land subsidence characteristics of Jakarta between 1997 and 2005, as estimated using GPS surveys. *Gps Solut.* **2008**, *12*, 23–32. [[CrossRef](#)]
174. Abidin, H.Z.; Andreas, H.; Gamal, M.; Gumilar, I.; Napitupulu, M.; Fukuda, Y.; Deguchi, T.; Maruyama, Y.; Riawan, E. Land subsidence characteristics of the Jakarta Basin (Indonesia) and its relation with groundwater extraction and sea level rise. In *Groundwater Response to Changing Climate*; CRC Press: Boca Raton, FL, USA, 2010; pp. 113–130.

175. Abidin, H.Z.; Andreas, H.; Gumilar, I.; Yuwono, B.D.; Murdohardono, D.; Supriyadi, S. On integration of geodetic observation results for assessment of land subsidence hazard risk in urban areas of Indonesia. *IAG 150 Years* **2015**, *143*, 435–442.
176. Hakim, W.L.; Achmad, A.R.; Eom, J.; Lee, C.-W. Land subsidence measurement of Jakarta coastal area using time series interferometry with Sentinel-1 SAR data. *J. Coast. Res.* **2020**, *102*, 75–81. [[CrossRef](#)]
177. Deltares, T. Sinking Cities: An Integrated Approach towards Solutions. Deltares–Taskforce Subsidence. 2011; p. 12. Available online: <https://publications.deltares.nl/Deltares142.pdf> (accessed on 20 December 2022).
178. Marfai, M.A.; King, L. Monitoring land subsidence in Semarang, Indonesia. *Environ. Geol.* **2007**, *53*, 651–659. [[CrossRef](#)]
179. Lubis, A.M.; Sato, T.; Tomiyama, N.; Isezaki, N.; Yamanokuchi, T. Ground subsidence in Semarang-Indonesia investigated by ALOS–PALSAR satellite SAR interferometry. *J. Asian Earth Sci.* **2011**, *40*, 1079–1088. [[CrossRef](#)]
180. Abidin, H.Z.; Andreas, H.; Gumilar, I.; Sidiq, T.P.; Gamal, M.; Murdohardono, D.; Supriyadi, Y.F. Studying land subsidence in Semarang (Indonesia) using geodetic methods. In Proceedings of the FIG Congress 2010, Sydney, Australia, 11–16 April 2010.
181. Hamdani, R.S.; Hadi, S.P.; Rudiarto, I. Progress or Regress? A Systematic Review on Two Decades of Monitoring and Addressing Land Subsidence Hazards in Semarang City. *Sustainability* **2021**, *13*, 13755. [[CrossRef](#)]
182. Yastika, P.; Shimizu, N.; Abidin, H. Monitoring of long-term land subsidence from 2003 to 2017 in coastal area of Semarang, Indonesia by SBAS DInSAR analyses using Envisat-ASAR, ALOS-PALSAR, and Sentinel-1A SAR data. *Adv. Space Res.* **2019**, *63*, 1719–1736. [[CrossRef](#)]
183. Jakarta is Shinknig at a Fast Rate. Available online: <http://print.kompas.com/baca/english/2016/03/18/Jakarta-Is-Sinking-at-a-Fast-Rate> (accessed on 22 March 2017).
184. Abidin, H.; Andreas, H.; Gamal, M.; Wirakusumah, A.; Darmawan, D.; Deguchi, T.; Maruyama, Y. Land subsidence characteristics of the Bandung Basin, Indonesia, as estimated from GPS and InSAR. *J. Appl. Geod.* **2008**, *2*, 167–177. [[CrossRef](#)]
185. Abidin, H.Z.; Andreas, H.; Gumilar, I.; Wangsaatmaja, S.; Fukuda, Y.; Deguchi, T. Land subsidence and groundwater extraction in Bandung Basin, Indonesia. *IAHS Publ.* **2009**, *20*, 145.
186. Abidin, H.Z.; Gumilar, I.; Andreas, H.; Murdohardono, D.; Fukuda, Y. On causes and impacts of land subsidence in Bandung Basin, Indonesia. *Environ. Earth Sci.* **2013**, *68*, 1545–1553. [[CrossRef](#)]
187. Du, Z.; Ge, L.; Ng, A.H.-M.; Zhu, Q.; Yang, X.; Li, L. Correlating the subsidence pattern and land use in Bandung, Indonesia with both Sentinel-1/2 and ALOS-2 satellite images. *Int. J. Appl. Earth Obs. Geoinf.* **2018**, *67*, 54–68. [[CrossRef](#)]
188. Sharifikia, M. Evaluation of land subsidence related disasters in plains and residential areas of Iran. *Iran. Assoc. Eng. Geol.* **2010**, *3*, 43–58.
189. Mahmoudpour, M.; Khamehchiyan, M.; Nikudel, M.R.; Ghassemi, M.R. Numerical simulation and prediction of regional land subsidence caused by groundwater exploitation in the southwest plain of Tehran, Iran. *Eng. Geol.* **2016**, *201*, 6–28. [[CrossRef](#)]
190. Amighpey, M.; Arabi, S.; Talebi, A.; Djamour, Y. *Elevation Changes of the PRECISE LEVELING tracks in the Iran Leveling Network*; Scientific Report; National Cartographic Center (NCC): Tehran, Iran, 2006.
191. Dehghani, M.; Zoej, M.J.V.; Hooper, A.; Hanssen, R.F.; Entezam, I.; Saatchi, S. Hybrid conventional and Persistent Scatterer SAR interferometry for land subsidence monitoring in the Tehran Basin, Iran. *ISPRS J. Photogramm. Remote Sens.* **2013**, *79*, 157–170. [[CrossRef](#)]
192. Foroughnia, F.; Nemati, S.; Maghsoudi, Y.; Perissin, D. An iterative PS-InSAR method for the analysis of large spatio-temporal baseline data stacks for land subsidence estimation. *Int. J. Appl. Earth Obs. Geoinf.* **2019**, *74*, 248–258. [[CrossRef](#)]
193. Mahmoudpour, M.; Khamehchiyan, M.; Nikudel, M.; Gassemi, M. Characterization of regional land subsidence induced by groundwater withdrawals in Tehran, Iran. *Geopersia* **2013**, *3*, 49–62.
194. Gatto, P.; Carbognin, L. The Lagoon of Venice: Natural environmental trend and man-induced modification/La Lagune de Venise: L'évolution naturelle et les modifications humaines. *Hydrol. Sci. J.* **1981**, *26*, 379–391. [[CrossRef](#)]
195. Carbognin, L.; Teatini, P.; Tosi, L. Eustacy and land subsidence in the Venice Lagoon at the beginning of the new millennium. *J. Mar. Syst.* **2004**, *51*, 345–353. [[CrossRef](#)]
196. Carbognin, L.; Gatto, P.; Mozzi, G.; Gambolati, G.; Ricceri, G. New Trend in the Subsidence of Venice. In *Land Subsidence Proceedings of II International Symposium on Land Subsidence, Anaheim, USA, 13–17 Demcember 1976*; IAHS: Wallingford, UK, 1976; Volume 121, pp. 65–81.
197. Carbognin, L.; Tosi, L.; Teatini, P. Analysis of actual land subsidence in Venice and its hinterland (Italy). In *Land Subsidence, Proceedings of the 5th International Symposium on Land Subsidence, Hague, The Netherlands, 16–20 October 1995*; International Association Hydrogeological Sciences: Wallingford, UK, 1995; pp. 129–137.
198. Carbognin, L.; Marabini, F.; Tosi, L. Land subsidence and degradation of the Venice littoral zone (Italy). In *Land Subsidence, Proceedings of the 5th International Symposium on Land Subsidence, Hague, The Netherlands, 16–20 October 1995*; International Association Hydrogeological Sciences: Wallingford, UK, 1995; pp. 391–402.
199. Teatini, P.; Gambolati, G.; Tosi, L. A new 3-D non-linear model of the subsidence of Venice. In *Land Subsidence, Proceedings of the 5th International Symposium on Land Subsidence, Hague, The Netherlands, 16–20 October 1995*; International Association Hydrogeological Sciences: Wallingford, UK, 1995; pp. 353–361.
200. Tosi, L. L'evoluzione paleoambientale tardo-quadernaria del litorale veneziano nelle attuali conoscenze. *Il Quat.* **1994**, *7*, 589–596.
201. Zanchettin, D.; Bruni, S.; Raicich, F.; Lionello, P.; Adloff, F.; Androsov, A.; Antonioli, F.; Artale, V.; Carminati, E.; Ferrarin, C. Sea-level rise in Venice: Historic and future trends. *Nat. Hazards Earth Syst. Sci.* **2021**, *21*, 2643–2678. [[CrossRef](#)]

202. Carbognin, L.; Gatto, P.; Mozzi, G.; Gambolati, G. Land subsidence of Ravenna and its similarities with the Venice case. In Proceedings of the Evaluation and Prediction of Subsidence, Pensacola Beach, FL, USA, 3–6 December 1978; pp. 254–266.
203. Carbognin, L.; Gatto, P.; Mozzi, G. Case history no.9.15: Ravenna, Italy. In *Guidebook to Studies of Land Subsidence due to Ground-Water Withdrawal*; Poland, J.F., Ed.; UNESCO: Paris, France, 1984; pp. 291–305.
204. Teatini, P.; Ferronato, M.; Gambolati, G.; Bertoni, W.; Gonella, M. A century of land subsidence in Ravenna, Italy. *Environ. Geol.* **2005**, *47*, 831–846. [[CrossRef](#)]
205. Bonsignore, F.; Bitelli, G.; Chahoud, A.; Macini, P.; Mesini, E.; Severi, P.; Villani, B.; Vittuari, L. Recent extensometric data for the monitoring of subsidence in Bologna (Italy). In Proceedings of the International symposium on land subsidence No8, Santiago de Querétaro, Mexico, 17–22 October 2010; pp. 333–338.
206. Molina, J.L.; García Aróstegui, J.L.; Benavente, J.; Varela, C.; de la Hera, A.; López Geta, J.A. Aquifers overexploitation in SE Spain: A proposal for the integrated analysis of water management. *Water Resour. Manag.* **2009**, *23*, 2737–2760. [[CrossRef](#)]
207. Herrera, G.; Tomás, R.; Monells, D.; Centolanza, G.; Mallorquí, J.; Vicente, F.; Navarro, V.; Sanchez, J.; Sanabria, M.; Cano, M.; et al. Analysis of subsidence using TerraSAR-X data: Murcia case study. *Eng. Geol.* **2010**, *116*, 284–295. [[CrossRef](#)]
208. Psimoulis, P.; Ghilardi, M.; Fouache, E.; Stiros, S. Subsidence and evolution of the Thessaloniki plain, Greece, based on historical leveling and GPS data. *Eng. Geol.* **2007**, *90*, 55–70. [[CrossRef](#)]
209. Svigkas, N.; Papoutsis, I.; Loupasakis, C.; Tsangaratos, P.; Kiratzi, A.; Kontoes, C. Land subsidence rebound detected via multi-temporal InSAR and ground truth data in Kalochori and Sindos regions, Northern Greece. *Eng. Geol.* **2016**, *209*, 175–186.
210. Loupasakis, C.; Sotiriadis, M.; Soulios, G. Hydrochemical characteristics of the underground water of the plain area located between Thessaloniki and N. Halkidona. In Proceedings of the 4th Hydrogeological Congress of the Hellenic Hydrogeological Committee and the Association of Geologists and Mineralogists of Cyprus; Hellenic Committee of Hydrogeology: Thessaloniki, Greece, 1997; pp. 194–212.
211. Rozos, D.; Apostolidis, E.; Xatzinakos, I. Engineering-geological map of the wider Thessaloniki area, Greece. *Bull. Eng. Geol. Environ.* **2004**, *63*, 103–108. [[CrossRef](#)]
212. Andronopoulos, V.; Rozos, D.; Hadzinakos, I. Subsidence phenomena in the industrial area of Thessaloniki, Greece. *Land Subsidi.* **1991**, *200*, 59–69.
213. Koumantakis, I.; Rozos, D.; Markantonis, K. Ground subsidence in Thermaikos municipality of Thessaloniki County, Greece. In Proceedings of the International Conference Gro-Pro–Ground water protection–Plans and Implementation in a North European Perspective, Korsør, Denmark, 15–17 September 2008; pp. 177–184.
214. Svigkas, N.; Loupasakis, C.; Papoutsis, I.; Kontoes, C.; Alatza, S.; Tzampoglou, P.; Tolomei, C.; Spachos, T. InSAR Campaign Reveals Ongoing Displacement Trends at High Impact Sites of Thessaloniki and Chalkidiki, Greece. *Remote Sens.* **2020**, *12*, 2396. [[CrossRef](#)]
215. Ganas, A.; Salvi, S.; Atzori, S.; Tolomei, C. Ground deformation in Thessaly, Central Greece, retrieved from Differential Interferometric analysis of ERS-SAR data. In Proceedings of the Abstract Volume of the 11th International Symposium on Natural and Human Induced Hazards & 2nd Workshop on Earthquake Prediction, Patras, Greece, 22–25 June 2006.
216. Salvi, S.; Ganas, A.; Stramondo, S.; Atzori, S.; Tolomei, C.; Pepe, A.; Manzo, M.; Casu, F.; Bernardino, P.; Lanari, R. Monitoring long-term ground deformation by SAR Interferometry: Examples from the Abruzzi, Central Italy, and Thessaly, Greece. In Proceedings of the 5th International Symposium on Eastern Mediterranean Geology, Thessaloniki, Greece, 14–20 April 2004; pp. 1–4.
217. Kontogianni, V.; Pytharouli, S.; Stiros, S. Ground subsidence, Quaternary faults and vulnerability of utilities and transportation networks in Thessaly, Greece. *Environ. Geol.* **2007**, *52*, 1085–1095. [[CrossRef](#)]
218. Fakhri, F.; Kalliola, R. Monitoring ground deformation in the settlement of Larissa in Central Greece by implementing SAR interferometry. *Nat. Hazards* **2015**, *78*, 1429–1445. [[CrossRef](#)]
219. Vassilopoulou, S.; Sakkas, V.; Wegmuller, U.; Capes, R. Long term and seasonal ground deformation monitoring of Larissa Plain (Central Greece) by persistent scattering interferometry. *Cent. Eur. J. Geosci.* **2013**, *5*, 61–76. [[CrossRef](#)]
220. Kaplanidis, A.; Fountoulis, D. Subsidence phenomena and ground fissures in Larissa, Karla basin, Greece: Their results in urban and rural environment. In Proceedings of the Proceedings of International Symposium on Engineering Geology and the Environment, Athens, Greece, 23–27 June 1997; pp. 23–27.
221. Rozos, D.; Sideri, D.; Loupasakis, C.; Apostolidis, E. Land subsidence due to excessive ground water withdrawal. A case study from Stavros-Farsala site, west Thessaly Greece. In Proceedings of the 12th International Congress of the Geological Society of Greece, Patras, Greece, 19–22 May 2010; Volume 43, pp. 1850–1857.
222. Kaitantzian, A.; Loupasakis, C.; Rozos, D. Assessment of geo-hazards triggered by both natural events and human activities in rapidly urbanized areas. In *Engineering Geology for Society and Territory*; Springer: Berlin/Heidelberg, Germany, 2015; Volume 5, pp. 675–679.
223. Kaitantzian, A.; Loupasakis, C.; Tzampoglou, P.; Parcharidis, I. Ground Subsidence Triggered by the Overexploitation of Aquifers Affecting Urban Sites: The Case of Athens Coastal Zone along Faliro Bay (Greece). *Geofluids* **2020**, *2020*, 8896907. [[CrossRef](#)]
224. Tzampoglou, P.; Loupasakis, C. Land subsidence due to the overexploitation of the aquifer at the Valtонера village. *Bull. Geol. Soc. Greece* **2017**, *50*, 1006. [[CrossRef](#)]

225. Tzampoglou, P.; Loupasakis, C. Land subsidence susceptibility and hazard mapping: The case of Amyntaio Basin, Greece. In Proceedings of the Fifth International Conference on Remote Sensing and Geoinformation of the Environment (RSCy2017), Paphos, Cyprus, 20–23 March 2017; p. 104441L.
226. Tzampoglou, P.; Loupasakis, C. Mining geohazards susceptibility and risk mapping: The case of the Amyntaio open-pit coal mine, West Macedonia, Greece. *Environ. Earth Sci.* **2017**, *76*, 542. [[CrossRef](#)]
227. Liu, Y.; Ma, T.; Du, Y. Compaction of muddy sediment and its significance to groundwater chemistry. *Procedia Earth Planet. Sci.* **2017**, *17*, 392–395. [[CrossRef](#)]
228. Li, Y.; Gong, H.; Zhu, L.; Li, X. Measuring spatiotemporal features of land subsidence, groundwater drawdown, and compressible layer thickness in Beijing Plain, China. *Water* **2017**, *9*, 64. [[CrossRef](#)]
229. Guzy, A.; Malinowska, A.A. State of the art and recent advancements in the modelling of land subsidence induced by groundwater withdrawal. *Water* **2020**, *12*, 2051. [[CrossRef](#)]
230. Huang, Z.; Yu, F. InSAR-derived surface deformation of Chaoshan Plain, China: Exploring the role of human activities in the evolution of coastal landscapes. *Geomorphology* **2023**, *426*, 108606. [[CrossRef](#)]
231. Herrera-García, G.; Ezquerro, P.; Tomás, R.; Béjar-Pizarro, M.; López-Vinielles, J.; Rossi, M.; Mateos, R.M.; Carreón-Freyre, D.; Lambert, J.; Teatini, P. Mapping the global threat of land subsidence. *Science* **2021**, *371*, 34–36. [[CrossRef](#)] [[PubMed](#)]
232. FAO. AQUASTAT—Global Map of Irrigation Areas. Food and Agriculture Organization of the United Nations (FAO). Available online: <https://www.fao.org/aquastat/en/geospatial-information/global-maps-irrigated-areas/index.html> (accessed on 1 February 2023).
233. Peng, M.; Lu, Z.; Zhao, C.; Motagh, M.; Bai, L.; Conway, B.D.; Chen, H. Mapping land subsidence and aquifer system properties of the Willcox Basin, Arizona, from InSAR observations and independent component analysis. *Remote Sens. Environ.* **2022**, *271*, 112894. [[CrossRef](#)]
234. Tang, W.; Zhao, X.; Motagh, M.; Bi, G.; Li, J.; Chen, M.; Chen, H.; Liao, M. Land subsidence and rebound in the Taiyuan basin, northern China, in the context of inter-basin water transfer and groundwater management. *Remote Sens. Environ.* **2022**, *269*, 112792. [[CrossRef](#)]
235. Ghorbani, Z.; Khosravi, A.; Maghsoudi, Y.; Mojtahedi, F.F.; Javadnia, E.; Nazari, A. Use of InSAR data for measuring land subsidence induced by groundwater withdrawal and climate change in Ardabil Plain, Iran. *Sci. Rep.* **2022**, *12*, 13998. [[CrossRef](#)] [[PubMed](#)]
236. Ciampalini, A.; Bardi, F.; Bianchini, S.; Frodella, W.; Del Ventisette, C.; Moretti, S.; Casagli, N. Analysis of building deformation in landslide area using multisensor PSInSAR™ technique. *Int. J. Appl. Earth Obs. Geoinf.* **2014**, *33*, 166–180. [[CrossRef](#)] [[PubMed](#)]

Disclaimer/Publisher’s Note: The statements, opinions and data contained in all publications are solely those of the individual author(s) and contributor(s) and not of MDPI and/or the editor(s). MDPI and/or the editor(s) disclaim responsibility for any injury to people or property resulting from any ideas, methods, instructions or products referred to in the content.